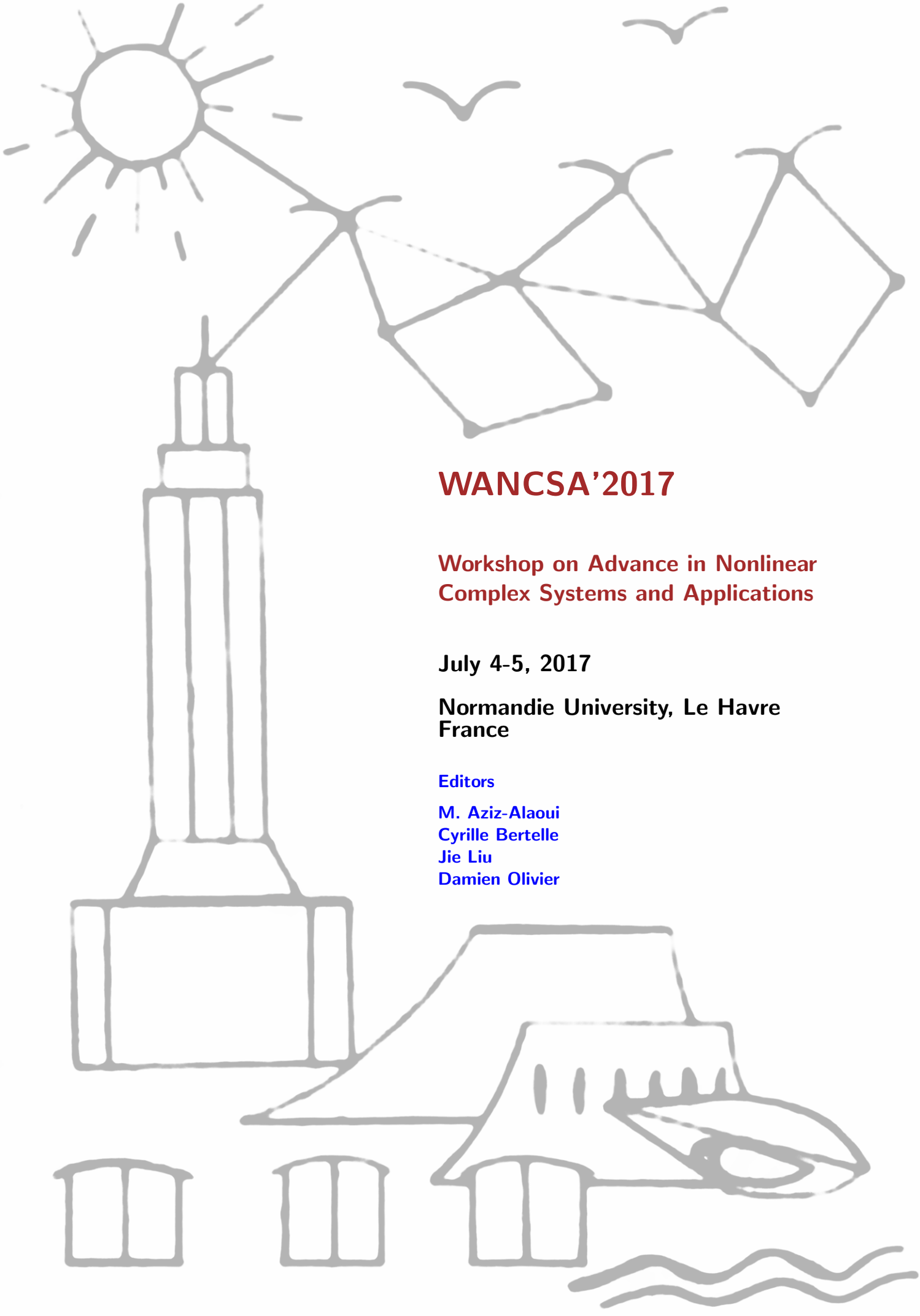

WANCSA'2017

Workshop on Advance in Nonlinear Complex Systems and Applications

July 4-5, 2017

Normandie University, Le Havre France

Editors

M. Aziz-Alaoui
Cyrille Bertelle
Jie Liu
Damien Olivier

WANCSA'2017

Workshop on Advance in Nonlinear Complex Systems and Applications

July 4-5, 2017

Normandie University, Le Havre
France

Editors
M. Aziz-Alaoui
Cyrille Bertelle
Jie Liu
Damien Olivier

This international event is organized by French and Chinese universities:

- LITIS, Laboratory of Computer Science, Information Processing and Systems, University Le Havre Normandie, University of Rouen Normandie & Insa Rouen Normandie, France
- LMAH, Laboratory of Applied Mathematics, University Le Havre Normandie, France
- LMI, Laboratory of Mathematics of Insa Rouen Normandie, France
- College of Mathematics and Computer Sciences, Wuhan Textile University, Wuhan, Hubei, P.R. China
- School of Mathematics and Statistics, Changsha University, Changsha, Hunan, P.R. China

The organizers thank for their scientific and financial supports:

- FNM CNRS-3335, Federation of Mathematics in Normandie, France
- NormaSTIC CNRS-3638, Federation of ICT in Normandie, France
- ISCN, Institute of Complex Systems in Normandy, France
- University Le Havre Normandie, France
- CS-DC UNESCO UniTwin, Complex System Digital Campus
- European Regional Development Fund - XTerM project

General Chairs:

- **M. AZIZ-ALAOUI**
  ISCN & LMAH
  University Le Havre Normandie
  25 Rue Ph. Lebon, BP 1123, 76063 Le Havre, France
  email: aziz.alaoui@univ-lehavre.fr
- **Cyrille BERTELLE**
  ISCN & LITIS
  University Le Havre Normandie
  25 Rue Ph. Lebon, BP 1123, 76063 Le Havre, France
  email: cyrille.bertelle@univ-lehavre.fr
- **Jie LIU**
  Research Centre of Nonlinear Science
  Wuhan Textile University
  Wuhan, Hubei, 430073, P.R. China
  email: liujie_hch@163.com
- **Damien OLIVIER**
  ISCN & LITIS
  University Le Havre Normandie
  25 Rue Ph. Lebon, BP 1123, 76063 Le Havre, France
  email: damien.olivier@univ-lehavre.fr

Program Committee:

Preface

Following the previous edition held in Wuhan-China (WTU), May 28-29, 2016, WANCSA'2017 will focus on recent advances in complex systems, complex networks, and applications in all fields of science and engineering. There will be several invited expository addresses covering recent trends and invited lectures on problems of current interest and important applications in various disciplines. Among surrounding areas of modelling capable of synthesizing the complexity of the systems, networks have well formalized mathematical bases which help in the operational effectiveness of these models; they are also an important vector of interdisciplinary reflection so much their presence seems obvious to represent the complex interlacing of various phenomena, natural, social and artificial systems.

They represent naturally systems of interaction between several parts. It is then frequent to see the emergence of collective behavior stemming from these parts in interaction.

Examples are many, whether it is in the natural world (nervous system, immune system, chains trophiques food, ...) or artificial (supply chain, cloud computing, internet, network social, ...) In which particular properties can emerge resulting from the interaction of the parts or from elements establishing the whole.

Complex networks are one of more powerful tools to describe, analyze and control all these natural or artificial complex systems, which are omnipresent. To understand and analyze them, new approaches based on integrative modellings are necessary.

Le Havre
July 4th 2017

M. Aziz-Alaoui
Cyrille Bertelle
Jie Liu
Damien Olivier

Contents

Proceedings of WANCSA 2017
Normandie University, Le Havre, France - July 3-4, 2014

RESEARCH ON DYNAMICS AND STRUCTURES' MUTUAL REPRESENTATION BETWEEN NONLINEAR TIME SERIES AND COMPLEX NETWORK GRAPHS

Jie Liu *

Abstract. In recent several years, several types of new mapping methods had been made to bridge the gap between time series and complex networks, which aims to study the usage of network features to depict geometry of different type of time series. Although some important studies have shown that, different types of time series is corresponding to different types of topological structure, but what relationship between these topology characters (ie.,the network characteristic quantities) and the original time series, is still unclear. So, how to apply the network analysis method to depict the characteristics of the original time series' statistics (vice versa the inverse process of such a research) therefore become extremely urgent nowadays. This talk recalled and addressed on the internal relationship between nonlinear time series and complex networks (duality of networks and time series) for further application research. It is suggested that two aspects of research should be further investigated on details, and the followed two aspects are also very urgent for real applications in near future: On one hand, network analysis method for time series from different sources depicting should be improved, and if possible, a unified framework for that should be established; On the other hand, a set of new and practical methods should be established based on classical time series analysis methods for describing the complex real networks via characterizations calculations. This field is a natural extension of current research focus on complex systems. Research in this direction will provide new methods and powerful tools, for analysis of the causal relationships between complex structures and temporal behaviors of a complex system, and as well as for structure and function analysis of a complex networks.

Keywords. Time series, Complex networks, Structure and function analysis, Duality of networks and time series, Graph theory

Brief Introduction

This talk will conclude several parts listed as follows:

- Some backgrounds of nonlinear time series analysis and complex networks analysis.
- Recent advance on duality analysis of networks and time series.
- Some applications of such duality analysis techniques.
- Brief conclusion and outlook.

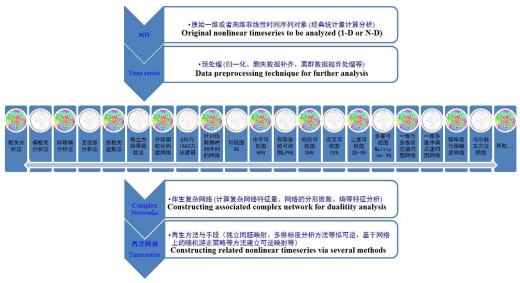

Figure 1: Main methods for map constructing between time series and networks, by J Liu et. al.

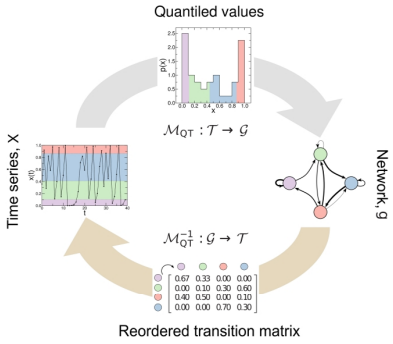

Figure 2: Illustration for duality between time series and networks, adopted from Ref. by Campanharo A S L O et. al.

Acknowledgements

The research for this work was supported partly by the Natural Sciences Foundation of China under grant number 61573011.

*Jie Liu is with Department of Mathematics, Wuhan Textile University, PR China, 430073; 2.Research Centre of Nonlinear Science (RCNS), Wuhan Textile University, PR China, 430073

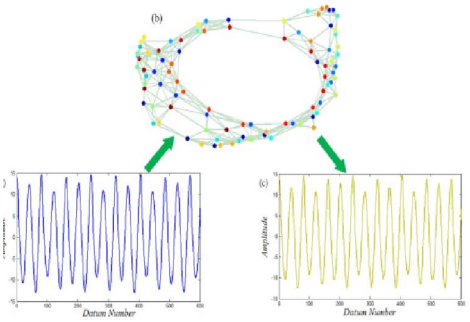

Figure 3: Illustration for geometrical invariability of transformation between a time series and a complex network, adopted from Ref. by Zhao Yi et. al.

References

[1]
- (a)L. Lacasa, B. Luque, F. Ballesteros, J. Luque and J.C. Nuno, From time series to complex networks: the visibility graph[J], Proc. Natl. Acad. Sci., 2008, 105(13), 4973.
- (b)A. M. Nunez, L. Lacasa, J. P. Gomez, B. Luque., Visibility algorithms: a short review, New Frontiers in Graph Theory[C], Edited by Zhang Yagang, 2012, Chapter 6, 2012: 119-152.
- (f)Gao Z-K Jin N-D., Complex network from time series based on phase space reconstruction[J], Chaos. 2009 , 19: 033137.
- (g)Gao Z-K, Hu Li-Dan, Zhou Ting-Ting et al. Limited penetrable visibility graph from two-phase flow for investigating flow pattern dynamics[J]. Acta Phys. Sin, 2013, 62(11): 110507.
- (h)Zhou Ting-Ting, JIN Ning-De, Gao Z-K et al. Limited penetrable visibility graph for establishing complex network from time series[J]. Acta Phys. Sin, 2012, 61(3): 030506.
- (i)Gao Z-K, Jin N-D., Wang W-X, Lai Y.-C., Motif distributions in phase-space networks for characterizing experimental two-phase flow patterns with chaotic features[J], Physical Review E,2010,82:016210.
- (j)Gao Z-K, Hu L-D, Jin N-D., Markov transition probability-based network from time series for characterizing experimental two-phase flow[J], Chin. Phys. B, 2013, 22, (5):050507.
- (k)Dong Zhao, Li Xiang. The study of network motifs induced from discrete time series[J]. Acta Phys. Sin., 2010, 59(3): 1600-1607.
- (l)Li Xiang, Dong Zhao, Detection and prediction of the onset of human ventricular fibrillation: An approach based on complex network theory[J], Phys. Rev. E, 84, pp. 062901, 2011.
- (m)Li Xiang, Yang Dong, Liu X., Wu X.M., Bridging time series dynamics and complex network theory with application to electrocardiogram analysis[J], IEEE Circuits and Systems Magazine, 2012, 12 (4):33-46.
- (n)Li Xiang, Liu Xin, Tse Chi K., Recent Advances in Bridging Time Series and Complex Networks[C], in Proceeding of 2012 IEEE International Symposium on Circuits and Systems (ISCAS), 2013:2505-2508.

[2]
- (a)Nicosia V, Lacasa L, Latora V., From multivariate time series to multiplex visibility graphs[J]. arXiv:1408.0925, 2014.
- (b)Lucas Lacasa, Vincenzo Nicosia and Vito Latora., Network structure of multivariate time series[J]. Sci. Rep. 5, 15508; doi: 10.1038/srep15508 (2015).
- (c) Gao Z K, Fang P C, Ding M S, et al. Multivariate weighted complex network analysis for characterizing nonlinear dynamic behavior in two-phase flow[J]. Experimental Thermal and Fluid Science, 2015, 60: 157-164.
- (d) Liu Jie, Li Q-Q. Planar visibility graph network algorithm for two dimensional timeseries[C], Proceeding of C-CDC2017, May.28, Chongqing, China, pp356-1361, 2017.
- (e) Liu Jie, Liu Hongling, Huang Zejia, and Tang Qiang., Differ multivariate timeseries from each other based on a simple multiplex visibility graphs technique[C], Proceeding of the Sixth Int. Conf. on Intelligent Control and Information Processing, Wuhan, China, Nov. 26-28, 2015, PP:290-295.

[3]
- (a)Marwan, N., Romano, M. C., Thiel, M., Kurths, J., Recurrence Plots for the Analysis of Complex Systems[J], Physics Reports, 2007, 438(5-6): 237-329.
- (b)Donner R.V, Zou Yong, J. F Donges, N Marwan and J Kurths, Recurrence networks - a novel paradigm for nonlinear time series analysis[J], New J. Phys, 2010. 12:033025.
- (c)Donner R.V, Small M, Donges JF, Marwan N, Zou Y, et al. Recurrence based time series analysis by means of complex network methods[J]. Int J of Bifur and Chaos. 2011, 21,(4):10191046.
- (d)J. F. Donges, J. Heitzig, R.V. Donner, J. Kurths., Analytical framework for recurrence network analysis of time series[J], Physical Review E, 2012 , 85, 4:046105.

[4]
- (a)S. Schinkel, N. Marwan and J. Kurths., Order Patterns Recurrence Plots in the Analysis of ERP Data[J], Cognitive Neurodynamics, 2007, 1(4):317-325.
- (b)S. Schinkel, G. Zamora-Lopez, O. Dimigen, W. Sommer and J. Kurths., Order Patterns Networks (ORPAN) - a method to estimate time-evolving functional connectivity from multivariate time series[J], Front. Comput. Neurosci. , 2012, 6:91.

[5]
- (a)Shirazi AH, Jafari GR, Davoudi J, Peineke J, Tabar M, Muhammad S., Mapping stochastic processes onto complex networks[J]. J of Statis Mech., 7, P07046, 2009.
- (b)Hirata, Y., Horai, S., Aihara, K., Reproduction of distance matrices and original time series from recurrence plots and their applications[J]. Eur. Phys. J. Special Topics, 2008,164:13-22.
- (c)Yutaka Shimada, T Ikeguchi, T Shigahara., From networks to time series[J], Phys Rev Lett., 2012, 109: 158701.
- (d)Liu Jie, Shi Shu-Ting, Zhao Jun-Chan., Comparison study of typical algorithms for reconstructing time series from the recurrence plot of dynamical systems[J]. Chinese Physics B. 2013, 22(1):010505.
- (e)Haraguchi Y, Shimada Y, Ikeguchi T, Aihara K, Transformation from complex networks to time series using classical multidimensional scaling[C], Proc of the 19th Int Conf on Artif Networks, Springer-Verlag. 2009.

[6]
- F. Strozzi., J. M. Zaldivar., K. Pioljansek, F. Bono., E. Gutierrez., From complex networks to time series analysis and viceversa: Application to metabolic networks[J], EUR-Scientific and Technical Research series. Luxembourg, 2009:1-56.
- Campanharo A S L O, Sirer M I, Malmgren R D, Ramos F M, Amaral L A N., Duality between Time Series and Networks[J]. PLoS ONE, 2011, 6 (8): e23378.
- Zhao Yi, Weng T F, Ye S., Geometrical invariability of transformation between a time series and a complex network[J]. Physical Review E, 2014, 90(1): 012804.

Proceedings of WANCSA 2017
Normandie University, Le Havre, France - July 3-4, 2014

ASSESSING THE OBSERVABILITY OF COMPLEX NETWORKS: A NONLINEAR THEORY

Christophe Letellier*& Irene Sendiña-Nadal†

Abstract. A network is said to be fully observable if its state can be discerned at any time from a subset of measured variables: this is a required property to safely investigate the underlying dynamics. Since a lack of observability is mainly associated with nonlinear couplings between variables, our approach consists in computing the observability coefficients from a so-called symbolic Jacobian matrix. We applied this approach to a reaction network, which encode the transformations of a chemical reaction, to determine the minimal set of variables and their derivatives to be measured for completing the state space reconstruction.

Keywords. Complex network, Observability, Control theory.

1 Introduction

Variables spanning the state space of a dynamical network are always dependent on each other through linear or nonlinear interactions. It is therefore no need to measure all of them for investigating the underlying dynamics. Our aim is to determine an adequate subset of variables together with their well-selected Lie derivatives to get a full observability of the network dynamics, that is, to accurately retrieve the network attractor [1, 2]. Complex networks are more and more often considered in various fields as well exemplified by power grids, socio-economics networks, or complex biological systems. A reliable monitoring, dynamical analysis or control of these high-dimensional networks, requires the development of some systematic techniques to identify such a subset of variables alowing the best (if not the full) observability. A related problem is how to unfold the dynamics by enlarging this subset of variables to reconstruct a space whose dimension is at least equal to the dimension of the original state space.

2 Observability

In order to quantify the observability, that is, the ability to distinguish states which are actually different in the original state space, let us consider a d-dimensional dynamical system $\dot{x}_i = f_i(\boldsymbol{x})$ where $\boldsymbol{x} \in \mathbb{R}^d$ is the state vector. The vector $\boldsymbol{s} \in \mathbb{R}^m$ of the m measured variables is provided by the measurement function $\boldsymbol{s} = h(\boldsymbol{x})$. One of the formal ways to define the observability of an autonomous system is as follows [3]. A dynamical system is said to be *state observable* at time t_f if every initial state $\boldsymbol{x}(0)$ can be uniquely determined from the knowledge of a finite time series of the measured variable $s(\tau)$, $0 \leq \tau \leq t_f$. It is possible to test whether the dynamical system is observable through a measurement function by investigating the rank of the observability matrix [4]

$$\mathcal{O} = \begin{bmatrix} \mathrm{d}h(\boldsymbol{x}) \\ \mathrm{d}\mathcal{L}_f h(\boldsymbol{x}) \\ \vdots \\ \mathrm{d}\mathcal{L}_f^{d-1} h(\boldsymbol{x}) \end{bmatrix} \tag{1}$$

where $\mathcal{L}_f^k$ is the kth Lie derivative. The Lie derivative of the ith component of the vector field $\boldsymbol{f}$ is defined as

$$\mathcal{L}_{f_i}(\boldsymbol{x}) = \sum_{k=1}^{d} \frac{\partial f_i(\boldsymbol{x})}{\partial x_k} f_k(\boldsymbol{x})\,. \tag{2}$$

The first (zeroth) order Lie derivative is thus the measured variable itself. The observability matrix $\mathcal{O}$ corresponds in fact to the Jacobian matrix of the change of coordinates $\Phi_{\boldsymbol{s}} : \mathbb{R}^d(\boldsymbol{x}) \to \mathbb{R}^d(\boldsymbol{X})$ where $\boldsymbol{X} \in \mathbb{R}^d$ is the reconstructed state vector made of the m measured variables and their appropriate $d-m$ Lie derivatives [5].

In order to avoid to test the rank of the Jacobian matrix via algebraic computation (something almost never possible to do when the dimension of the system becomes too large), we propose to use a technique based on a symbolic computation of the observability matrix in which the terms are not explicitely expressed but whose nature (linear, nonlinear polynomial or rational) is only considered: the procedure is detailed in [2, 6].

3 A 13D reaction network

A 13-dimensional rational reaction network describing the cell cycle during the fission of the yeast [7] is here investigated. Its Jacobian matrix $\mathcal{J}_f = (J_{ij})$ is transformed

*Christophe Letellier is Professor at Rouen University, France and member of CORIA. E-mails: Christophe.Letellier@coria.fr

†Irene Sendiña-Nadal is Associate Professor at Rey Juan Carlos University, Madrid, Spain, and member of the CTB, Technical University of Madrid. E-mail: irene.sendina@urjc.es

into the symbolic Jacobian matrix $\tilde{\mathcal{J}}_f = (\tilde{J}_{ij})$

$$\begin{bmatrix}
\bar{1} & \bar{1} & 0 & 1 & 0 & 0 & 0 & 1 & 0 & 0 & 0 & 0 & 0 \\
\bar{1} & \bar{\bar{1}} & \bar{1} & 1 & 0 & 0 & 0 & \bar{1} & 1 & 1 & 0 & 0 & \bar{1} \\
0 & \bar{1} & \bar{1} & 0 & 0 & 0 & 0 & 0 & 1 & 0 & 0 & 0 & 0 \\
\bar{1} & \bar{1} & 0 & 1 & 0 & 0 & 0 & 0 & 0 & 0 & 0 & 0 & 0 \\
\bar{1} & 0 & 0 & 0 & \bar{\bar{1}} & 0 & 0 & \bar{1} & 0 & 0 & 0 & 0 & 0 \\
\bar{1} & 0 & 0 & 0 & 0 & \bar{\bar{1}} & 0 & \bar{1} & 0 & 0 & 0 & 0 & 0 \\
\bar{1} & 0 & 0 & 0 & 0 & 0 & \bar{\bar{1}} & \bar{1} & 0 & 0 & 0 & 0 & 0 \\
1 & \bar{1} & 0 & 0 & 0 & 0 & 0 & \bar{1} & 0 & 1 & 0 & 0 & 0 \\
0 & \bar{1} & \bar{1} & 0 & 0 & 0 & 0 & 0 & 1 & 0 & 0 & 0 & 0 \\
0 & \bar{1} & 0 & 0 & 0 & 0 & 0 & \bar{1} & 0 & 1 & 0 & 0 & 0 \\
0 & 0 & 0 & 0 & \bar{1} & 0 & 0 & 0 & 0 & 0 & \bar{\bar{1}} & 0 & 0 \\
\bar{1} & 0 & 0 & 0 & 0 & 0 & 0 & \bar{1} & 0 & 0 & 0 & \bar{\bar{1}} & 0 \\
0 & 0 & 0 & 0 & 0 & 0 & 0 & 0 & 0 & 0 & 0 & 0 & 1
\end{bmatrix} \quad (3)$$

by replacing each linear element J_{ij} by 1, each non-linear polynomial element J_{ij} by $\bar{1}$, and each rational element J_{ij} by $\bar{\bar{1}}$ whenever the jth variable appears in the denominator or by $\bar{1}$ otherwise.

The number of times the ith variable occurs in linear terms in the governing equations of the system is equal to the linear out strength $\sigma^{\rm l}_{\rm out}(i)$ of the ith variable, that is, the number of elements $\tilde{J}_{ij}$ equal to one in the ith column of the symbolic jacobian matrix whose diagonal is removed. The larger the $\sigma^{\rm l}_{\rm out}(i)$, the more likely the ith variable is not to be measured. According to our linear out-strength $\sigma^{\rm l}_{\rm out}$, we have five candidate variables to be non-measured since

$$\sigma^{\rm l}_{\rm out}(1) = \sigma^{\rm l}_{\rm out}(8) = 1 < \sigma^{\rm l}_{\rm out}(4) = \sigma^{\rm l}_{\rm out}(9) = \sigma^{\rm l}_{\rm out}(10) = 2.$$

The linear off-diagonal elements ($\tilde{J}_{ij} = 1$) are $\tilde{J}_{14}$, $\tilde{J}_{18}$, $\tilde{J}_{24}$, $\tilde{J}_{29}$, $\tilde{J}_{2-10}$, $\tilde{J}_{39}$, $\tilde{J}_{81}$, and $\tilde{J}_{89}$. There is therefore a single pair of exclusive candidate variables, that is, variable x_1 and x_8 ($\tilde{J}_{18} = \tilde{J}_{81} = 1$). Variables x_1, x_9, and x_{10} can therefore be removed from the set of measured variables. The non-measured in-strength $\sigma^{\rm nm}_{\rm in}$ are equal to 2 for the five candidate variables. Our criterion does not allow us to determine which variable out of the five candidates can be discarded.

When we choose one of the candidate variables to not be measured, we obtained a full observability. When one of the variables x_6, x_7, x_{11} and x_{12} is removed from the the set of measured variables, the symbolic observability coefficient was equal to zero for any possible combination of their first derivative: these variables must therefore to be measured. In fact, these four variables have no inconnection other than with themselves, as easily deduced from the symbolic Jacobian matrix (3) of the DNA model.

Right after we checked whether it was possible to retrieve a full observability from our two potential sets of variables to not be measured, namely $\{x_1, x_4, x_9, x_{10}\}$ and $\{x_4, x_8, x_9, x_{10}\}$. For instance, the reconstructed state vectors

$$(x_1, \dot{x}_1, x_2, \dot{x}_2, x_3, \dot{x}_3, x_4, x_5, x_6, x_7, x_{11}, x_{12}, x_{13})$$
$$(x_1, \dot{x}_1, x_2, \dot{x}_2, x_3, x_4, x_5, x_6, x_7, x_{10}, x_{11}, x_{12}, x_{13})$$
$$(x_1, \dot{x}_1, x_2, x_3, \dot{x}_3, x_4, x_5, x_6, x_7, x_{10}, x_{11}, x_{12}, x_{13})$$

provide a full observability. When 9 variables are measured, the largest value for the symbolic observability coefficient we get is equal to 0.93, a sufficiently high value to ensure a very good observability of the original state space (a value of 0.75 is the estimated threshold for a good observability [8]). Therefore, it seems useless to explore into smaller sets of measured variables because the observability of the original state space will be no longer sufficient to allow a good discrimination between the different states of the system. We observed that by measuring only five with only five variables , the symbolic observability coefficient was already zero. In Fig. 1 we report how the observability of the original state space depends on the cardinality of the set of measured variables.

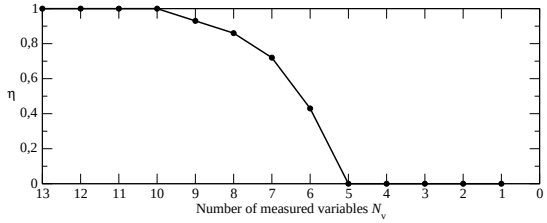

Figure 1: Largest symbolic observability coefficient η *versus* the number $N_{\rm v}$ of measured variables for the DNA model.

This is an important intermediate step before addressing larger complex networks.

Acknowledgements

Work partly supported by the Spanish Ministry of Economy under project FIS2013-41057-P.

References

[1] L. A. Aguirre, and C. Letellier, "Observability of multivariate differential embeddings," *Journal of Physics A*, vol. 38, pp. 6311-6326, 2005.

[2] E. BiancoMartinez, M. S. Baptista, and C. Letellier, "Symbolic computations of non-linear observability," *Physical Review E*, vol. 91, 062912, 2015.

[3] T. Kailath, *Linear Systems*, Prentice Hall, Englewood Cliffs, 1980.

[4] R. Hermann, and A. Krener, "Nonlinear controllability and observability," *IEEE Transactions on Automatic Control*, vol. 22, pp. 728-740, 1977.

[5] C. Letellier, L. A. Aguirre, and J. Maquet, "Relation between observability and differential embeddings for nonlinear dynamics," *Physical Review E*, vol. 71, 066213, 2005.

[6] C. Letellier, I. Sendiña-Nadal, E. Bianco-Martinez, and M. S. Baptista, "Assessing observability of reaction networks by using nonlinear symbolic coefficients," *preprint.*

[7] B. Novak, and J. J. Tyson, "Modeling the control of DNA replication in fission yeast,((*Proceedings of the National Academy of Science* (USA), vol. 94, pp. 9147-9152, 1997.

[8] I. Sendiña-Nadal, S. Boccaletti, and C. Letellier, "Observability coefficients for predicting the class of synchronizability from the algebraic structure of the local oscillators," *Physical Review E*, vol. 94, 042205, 2016.

Proceedings of WANCSA 2017
Normandie University, Le Havre, France - July 4-5, 2017

SELF-LOCALIZATION OF ANONYMOUS ROBOTS FROM AERIAL IMAGES

Olivier Poulet, François Guérin and Frédéric Guinand *†

Abstract

This paper presents three different methods for the localization of identical robots thanks to aerial pictures available at regular time intervals. Robots are anonymous, they do not have any identifier allowing self-identification and they cannot communicate with each others. Robots are moving in their environment. The proposed localization methods rely on these movements, through the analysis of angular or distance variations. Simulation is used for the evaluation of the methods.

1 Introduction

Robots localization is of key importance for cooperative control [1]. In multi-robots systems, when robots use the positions of others robots to compute their own position, the problem is called *cooperative localization* [2]. In [4] the authors express the difference between *relative mutual positions* and *absolute mutual localization* depending on robot's frame, if they are fixed or moving. In most works about cooperative localization methods, robots are not anonymous. In the works of Franchi & al, robots are anonymous. In [3] the authors develop an algorithm based on a particle filter to compute relative mutual positions, however, robots have the ability to communicate with each other to send and received poses with an index.

In our work, we assume that an aerial camera is available and it takes, periodically, pictures of a fixed area where all the robots are present. All robots are identical and are unable to communicate with each others. Their initial position is unknown. They have odometric sensors to mesure their rotation and linear speed. Camera sends to the robots, at regular intervals, pictures of the area on which all the robots appear, as illustrated on Figure 1. Camera is the single point of centralization. The challenge, for each robot, is to localize itself on the pictures. In the second part, the three formulations for localization are described, experiments and results are presented in, respectively, the third and the last part.

*Olivier Poulet and Frédéric Guinand are with LITIS laboratory, Normandy University of Le Havre, France. E-mails: pouletolivier@yahoo.fr, frederic.guinand@univ-lehavre.fr

†François Guérin is with GREAH laboratory, Normandy University of Le Havre, France. E-mail: francois.guerin@univ-lehavre.fr

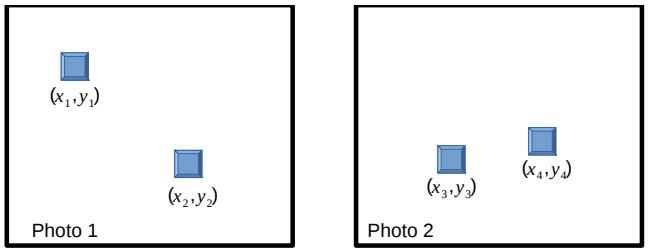

Figure 1: All robots receive, at regular time intervals, the same pictures and compute the coordinates of all anonymous robots. The question is: who am I?

2 Problem formulation

2.1 Angular variation

This first method is the simplest. It is necessary that camera can mesure positions and orientations of each robot. The localization begins with the reception of a first picture (date t_1). Each robot r records all the orientations θ_{i_r} of all the robots. At the same time, each robot realizes a random constant rotation in the same sense until the reception of the second picture (date t_2). Then, each robot records again the angles $\theta_{f_r} f$ of all the robots. Each robot knows its own rotation speed ω between the two dates. Robot r compares $\omega.(t_2 - t_1)$ with $\theta_{f_r} - \theta_{i_r}$ in order to estimation its position.

2.2 linear speed variation

This method uses the Pinhole camera model. Camera has its coordinate system and a image plane parallel to axes X and Y. Robots moved on a floor plan. It is assumed that the two plans are parallel as illustrated on Figure 2.

One Robot m wants to realize its self-localization among n robots. When it receives picture 1, it realizes a linear move at a random speed until the reception of picture 2. The robot realizes the distance R to R' (d_0). Between pictures 2 and 3, the robot moves again linearly at a different random speed. The robot m realized the distance R' R"(d_1). The projection distances on the camera plane are d'_0 and d'_1. The robot knows its ratio $a = \frac{d_0}{d_1}$, and with Thales theorem it comes that $a = \frac{d'_0}{d'_1}$. Finding the robot positions on each of the three pictures consists

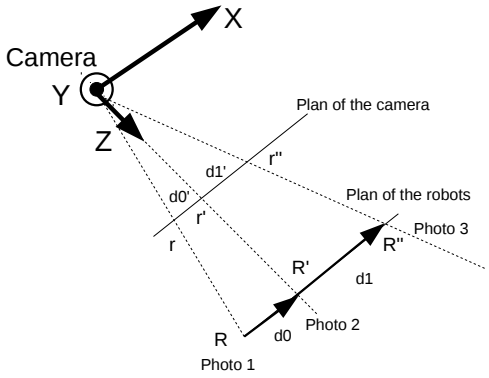

Figure 2: A robot realizes a linear motion between positions R, R', R", coordinates on pictures 1, 2, 3 and r, r', r" the projections on the camera plane.

in finding $min|a-r|$, where r is a matrix (dimension (n^3)) of all the possible ratios for all the distances between the 3 pictures. It is possible to reduce the matrix dimension r if we consider the linearity of 3 points from 3 pictures (dimension becomes n).

2.3 Localization during a random motion

N robots move according to differents trajectories. For expressing their movement we use the Char model:

$$\begin{pmatrix}\dot{x}\\ \dot{y}\\ \dot{\theta}\end{pmatrix} = \begin{pmatrix}\cos(\theta) & 0\\ \sin(\theta) & 0\\ 0 & 1\end{pmatrix} . \begin{pmatrix}v\\ r\end{pmatrix}$$

x, y are the coordinates of robots, θ represents the difference between speed angular vector and X axis, v and r are respectively the linear and the rotation speeds.

The movement of the robot between two positions is illustrated in Figure 3.

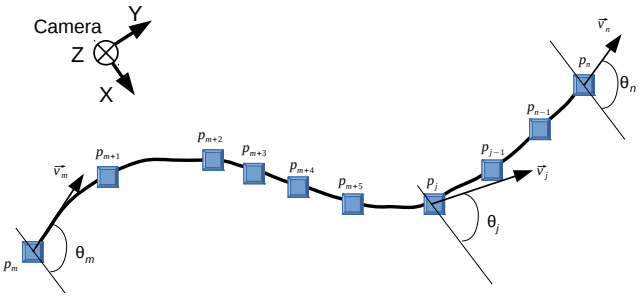

Figure 3: Robots positions from place p_m to p_n with intermediate positions p_j discretized

Using the Taylor tranformation $f(x_0+h) = f(x_0) + hf'(x_0) + h\epsilon(h)$, we prove that Char model becomes:

$$\begin{pmatrix}x_n - x_m\\ y_n - y_m\end{pmatrix} = \delta t \sum_{j=m+1}^{n} \begin{pmatrix}\lambda.\cos(\theta_m + \delta t \sum_{k=m+1}^{j} r_k)\\ \lambda.\sin(\theta_m + \delta t \sum_{k=m+1}^{j} r_k)\end{pmatrix} v_j$$

δt is the discretization time and we assume that $\lambda = \frac{f}{Z}$ in Pinhole model is known. The only unknown variable is θ_m. This means that if there is an existing identical θ_m for two coordinates between two consecutive pictures, we know the initial and final coordinates of the robot. We have solved this system for the self-localization only with two consecutive pictures.

3 Main results

To experiment the methods, we used the multi-robot simulator Player-stage and augmented reality software Artoolkit to determine coordinates. We tested only with 2 anonymous robots. The frequency of pictures was 10 seconds.

Self-localization Method	sucess rate
Angular variation	96.9%
linear speed variation*	84%
localization during motion	83.9%

* we have considered the linearity movement between 3 pictures.

4 Conclusion

We have presented three methods for self-localization in a multiple anonymous robots system. We have showed that the three methods have a success rate greater than 80%. Each of these methods have advantages and disadvantages, but in all the cases, robots received all of the anonymous coordinates set of the multi-robots system.

References

[1] J. Spletzer, A.K. Das, R. Fierro, C.J. Taylor, V. Kumar and J.P. Ostrowski, *Cooperative Localization and Control for Multi-Robot Manipulation*, Procesing of the IEEE/RSJ International Conference on Intelligent Robots and Systems(IROS), 2001.

[2] D. Fox, W. Burgard, H. Kruppa and S. Thrun, *A probabilistic approach to collaborative multi-robot localization*, Auton. Robots, vol. 8, no. 3,pp. 325-344, 2000.

[3] A. Franchi ,G. Oriolo and P. Stegagno, *Mutual Localization in a Multi-Robot System with Anonymous Relative Position Measures*, IEEE/RSJ Int.Conf. on Intelligent Robots and Systems, St. Louis, MO, pp 3974-3980, 2009.

[4] A. Franchi ,G. Oriolo and P. Stegagno, *Probabilistic Mutual Localization in Multi-Agent Systems from Anonymous Position Measures*, 49th IEEE Conf. on Dcision and Control, Atlanta, GA, pp 6534-6540, 2010.

Proceedings of WANCSA 2017
Normandie University, Le Havre, France - July 4-5, 2017

EXPLORING CHAOTIC DYNAMICS BY PARTITION OF BIFURCATION DIAGRAM

Boonyarit Changaival*, Martin Rosalie†

Abstract. Chaotic dynamical systems have been recently successfully used to replace uniform probability functions in several algorithms in optimization and machine learning. In this work, we propose a study on the use of bifurcation diagrams and first return map in the Rössler system for producing chaotic dynamics. Then, we plan to use these chaotic dynamic for optimization problem. With a bifurcation diagram we can also distinguish the periodic solutions apart from the chaotic solutions. By studying the chaotic solutions, we can then achieve a first return map which is a signature of the dynamical system and throughly study the complexity of the latter with a certain set of parameters. As a result, the partition in the bifurcation diagram is provided. From the first return maps, we are able to confirm the complexity of the dynamics in those partitions along with the transitions between them.

Keywords. Bifurcation Diagram, Chaotic Dynamics, First Return Map, Rössler System, Uniform Random Function

1 Related works

Rössler system was first introduced as a system for studying chemical reactions [4]. The system is defined by three differential equations:

$$\begin{cases} \dot{x} = -y - z \\ \dot{y} = x + ay \\ \dot{z} = b + z(x - c) \, . \end{cases} \tag{1}$$

The solutions that are retrieved from the system can be an attractor (chaotic solution) or a periodic solution. The first derivative $\dot{x}$, $\dot{y}$ and $\dot{z}$ is the definition of the problem where the x, y and z are the variables of the system; all variables at $t = 0$ are called initial conditions. A series of variables x, y and z from $t = 0 \rightarrow \infty$ is the solution of the system. Lastly, a, b and c are parameters to alter the behavior of the system. Regarding the parameters, Sprott and Li [5] proposed a method to generalize these parameters (a, b and c) modification with α as seen in:

$$\begin{cases} a = 0.2 + 0.09\alpha \\ b = 0.2 - 0.06\alpha \\ c = 5.7 - 1.18\alpha \, . \end{cases} \tag{2}$$

*Boonyarit Changaival is with Faculty of Science, Technology and Communication (FSTC-CSC), University of Luxembourg, Luxembourg. E-mail: boonyarit.changaival@uni.lu

†Martin Rosalie is with Interdisciplinary Centre for Security, Reliability and Trust (SnT), University of Luxembourg, Luxembourg. E-mail: martin.rosalie@uni.lu

From this parametrization, it has been shown that the system can only generate attractors with the same dynamics, i.e., with no more than three branches Fig. 1 (readers are encouraged to consult [3] for further details).

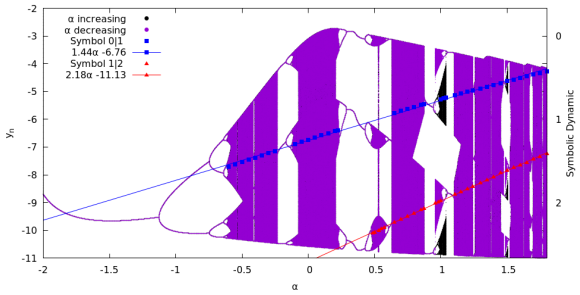

Figure 1: The bifurcation diagram where α is varied in Eq. (2) for the Rössler system Eq. (1).

The purpose of our work is to obtain more complex chaotic dynamics from this bifurcation diagram by using the banded chaos parts. We expect to improve algorithm performances by introducing these type of chaotic behavior.

2 Bifurcation Diagram Partition

A bifurcation diagram can be used as a tool to illustrate the behavior of each state in a chaotic dynamical system when a parameter is varied. This bifurcation diagram can only be obtained after the system discretization. We used the Poincaré section to complete this task.

The bifurcation diagram of the Rössler system with $\alpha = [-0.5, 1.2]$ is presented in Fig. 2. It can be clearly observed that there are three kinds of areas in the diagram. The first kind is a very sparse area, e.g. in the period of $\alpha = [0.3, 0.4]$. These values of α give periodic solutions. The second kind is a dense area, e.g. the period of $\alpha = [-0.1, 0.2]$. These α yield chaotic solutions. The third kind is a dense area with a gap, e.g. the period of $\alpha = [1.1, 1.15]$. The attractor yielded from these α is called "Banded Chaos". The characteristic of the banded chaos is more complex than previously mentioned chaotic attractors. Readers who would like to pursue further details should refer to [3].

We compute our first return maps with this equation:

$$\rho_n = (y_n - UB)/(LB - UB) \tag{3}$$

where LB stands for "Lower Bound" and UB is for "Upper Bound". These upper bound and lower bound are based on the bifurcation diagram. As shown in Fig. 2, the bifurcation diagram does not have a linear shape. Therefore, the diagram has been divided into several parts to ensure that we extract the values of ρ_n in $[0, 1]$ and retrieve non-equivalent dynamics from the bifurcation diagram. This is because the Rössler dynamics can be considered similar as a whole using templates and subtemplates according to [3]. LB and UB in Eq. (3) can be found in Eq. (4) and Eq. (5) respectively. In this work, we provide the partitions of $\alpha = [-0.5, 1.2]$ since the period of $\alpha < -0.5$ are mostly periodic and not entirely our focus.

$$LB = 0.110626 \times \alpha^2 - 10.585 + 0.4141 \times \alpha \tag{4}$$

$$UB = \begin{cases} 6.04162\alpha - 2.8 & \text{if } \alpha = [-0.5, -0.22] \\ -7.16446\alpha^2 + 3.31662\alpha - 3.05252 & \text{if } \alpha = (-0.22, 0.192] \\ -0.99127\alpha - 2.49 & \text{if } \alpha = (0.192, 0.790) \\ -4.31521\alpha - 4.01651 & \text{if } \alpha = [0.790, 0.876] \\ -0.99127\alpha - 2.49 & \text{if } \alpha = (0.876, 1.102) \\ 23.673\alpha - 34.2435 & \text{if } \alpha = [1.102, 1.155] \\ -0.99127\alpha - 2.49 & \text{if } \alpha = (1.155, 1.2] \end{cases} \tag{5}$$

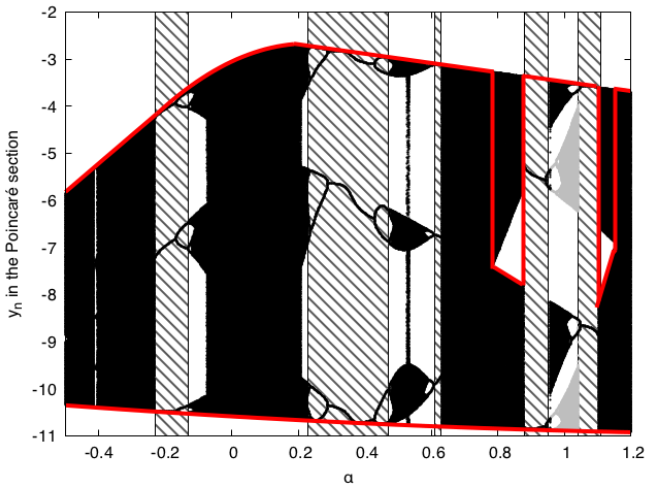

Figure 2: The bifurcation diagram with the upper and lower bounds.

A first return map is a dynamical signature of a system under an influence of a set of parameters. In the case of our work, the parameter is α. The map is drawn from a plot of ρ_n against ρ_{n+1} obtained from the partitions. The first return map does not only help in discerning whether the state of system is periodic or chaotic, but also aids in studying the complexity of the system behavior through the concept of branch in the first return map as described in [3]. The difference can be seen in Fig. 3 and Fig. 4, where our partition is not applied in the former, but the latter for the same value of α. Thus, a first return map with four branches (more complex) is obtained.

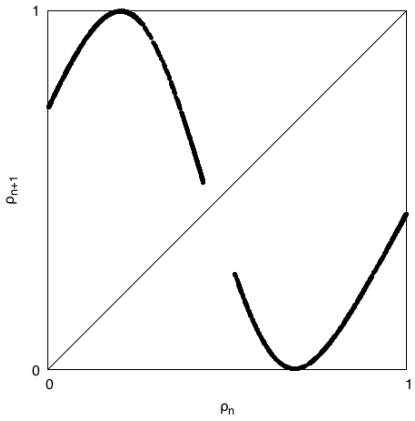

Figure 3: First Return Map of $\alpha = 1.135$ when the whole bands of "Banded Chaos" is considered.

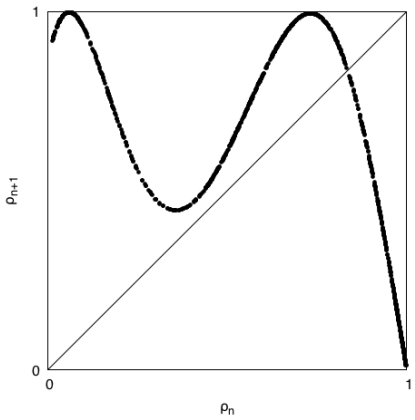

Figure 4: First Return Map of $\alpha = 1.135$ when only a lower band of "Banded Chaos" is considered.

3 Conclusion

In this paper, we provide a novel partition method that can extract high complexity behaviors from a banded chaotic attractor through a bifurcation diagram in the Rössler system. As future work, we aim to deploy the Rössler system in optimization algorithms such those that appeared in [1, 2] and graph traversal algorithm.

References

[1] A. H. Gandomi, X.-S. Yang, S. Talatahari, and A. Alavi. Firefly algorithm with chaos. *Communications in Nonlinear Science and Numerical Simulation*, 18(1):89–98, jan 2013.

[2] D. Liu and G. Chen. Hybrid algorithm for ant colony optimization based on chaos technique. In *Proc. of IEEE International Conference on Natural Computation*, volume 5, pages 2628–2632, 2010.

[3] M. Rosalie. Templates and subtemplates of Rössler attractors from a bifurcation diagram. *Journal of Physics A: Mathematical and Theoretical*, 49(31):315101, jun 2016.

[4] O. E. Rössler. An equation for continuous chaos. *Physics Letters A*, 57(5):397–398, 1976.

[5] J. Sprott and C. Li. Asymmetric bistability in the Rössler system. *Acta Physica Polonica B*, 48(1):97, 2017.

Proceedings of WANCSA 2017
Normandie University, Le Havre, France - July 3-4, 2017

TURING'S THEORY OF MORPHOGENESIS APPLIED TO STREET LAYOUT, FIRST APPROACH

Stefan Balev, Antoine Dutot, Damien Olivier and Michele Tirico *

Abstract. Urban morphology tries to understand the spatial structure of cities. It searches to identify the patterns and underlying substructures but also the process of city development. Our contribution follows this last direction. We model the development process of graphs representing the streets network using Turing model.
Keywords. Graphs, Morphogenesis, Cities, Complex sociotechnical Systems

1 Introduction

Cities are complex sociotechnical systems [1] constituted by a very large number of heterogeneous entities which evolve and interact. Urban morphology tries to understand the spatial structure of cities. It searches to identify the patterns and underlying substructure but also the process of city development. In a first time, we consider the structure and the development of the road network that define the street layout of our towns. We know that this approach is reductionist, anyway streets give structure of our cities and we hope that the model we incrementally develop could evolve with the complexity.

The problem consist to generate graphs under constraints which are spatially and temporally coherent. The constraints influence (facilitate or impede) the development of the graph.

In 1952, Alan Turing has considered the striping patterns than we can observed for example on the tiger pelage (see figure 1). His hypothesis was that a mechanism of reaction/diffusion [2] was at the origin of the structures present in certain biological tissues. It is a chemical process with two morphogens: an activator and an inhibitor.

We revisit this model to generate graphs showing structures.

2 Turing Model

Turing has imagined a chemical mechanism composed of two morphogens, an activator `A` and an inhibitor `I` that diffuse and react with each other. The environment is homogeneous. The activator `A` favors its own formation and diffuses slowly. The production of the inhibitor `I` is stimulated by `A`. I diffuses rapidly and inhibits the formation of `A`. This mechanism generates patterns.

Figure 1: Credit: J. Patrick Fischer / Wikimedia Commons / Public Domain

$$\begin{cases} \dfrac{\partial A}{\partial t} = F(A,I) - d_A I + D_A \Delta A \\ \dfrac{\partial I}{\partial t} = G(A,I) - d_I A + D_I \Delta I \end{cases}$$

Production — Degradation — Diffusion

Reaction

The initial conditions are a random uniform distribution of the two morphogens.

Since A is an autocatalyst and diffuses slowly, it stimulates production of itself and it concentrates into a peak. In the same time A boosts production of its inhibitor `I` which diffuses more quickly than itself. A concentrations decrease around the peak. At a sufficiently large distance from the peak, the influence of the inhibitor is too low and a peak appears. Turing explains in his paper [2] that a such system yields six potential stable states, depending on the production and degradation of reaction terms and wavelength of the pattern. One of them (type 6 in the original paper) shows stationary waves with finite wavelength (see figure 2).

*Normandie Univ, UNIHAVRE, LITIS, 76600 Le Havre, France. emails : subname.name@univ-lehave.fr

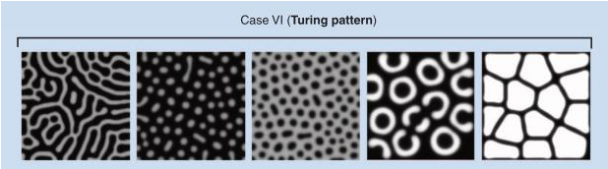

Figure 2: Two-dimensional patterns generated by the Turing model. These patterns were made by an identical equation with slightly different parameter values. Source: [3]

3 Coupling Turing Model and Graph

The simulation model is simple. There is a grid which represents the space where the reaction take place. The space is discretised. Each cell contains an amount of inhibitor and activator. For one step, the process is the following :

```
to Execute
  Production
  Degradation
  Diffusion
  WhatColor
end
```

The activator has a color C_a and when the activator concentration is above a threshold the cell is colored by C_a. This algorithm produces two-dimensional patterns (see figure 3).

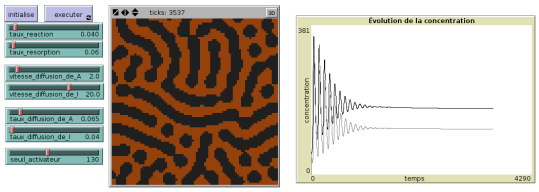

Figure 3: Netlogo simulation of Turing Model

Our model is a model with two levels. The first one is the Turing model and the second one is a temporal graph generated by the morphogenesis process (see figure 4). A node is created when the activator concentration is greater than a threshold. The creation retroacts on the first level by accelerating degradation of the activator and the production of the inhibitor. Different strategies are studied. The nodes are connected with their spatial neighbours.

4 Conclusion

This work is in progress. We have to study the parameter space. Anayway, we think that the concept of morphogenesis offers a new dimension to the urban study: the time, considered here as a dynamic continuum rather than as a result of a succession of distinct states. The morphogenesis tries to capture the organizational laws underlying the existence and development of urban forms. We have also to define a third level representing the streets layout (curves, intersections ...).

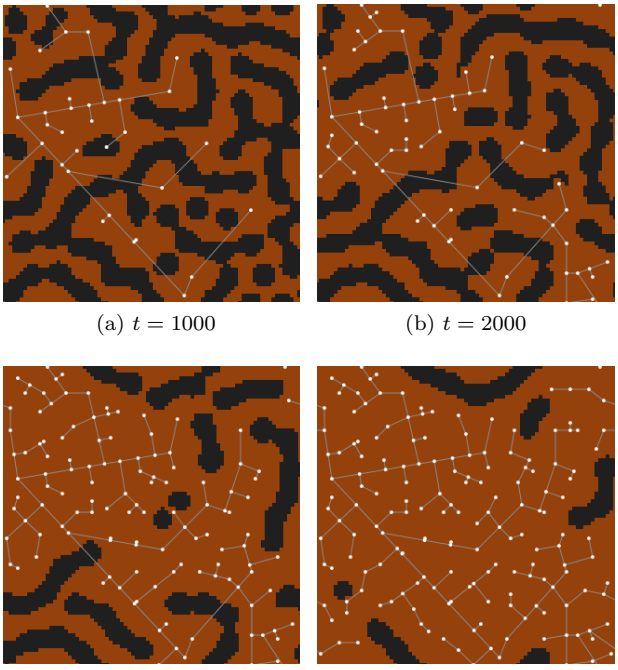

(a) $t = 1000$ (b) $t = 2000$

(c) $t = 4000$ (d) $t = 6000$

Figure 4: Example of Turing model coupled with a graph

Acknowledgements

The financial support of the FEDER through the project grant AMED is gratefully acknowledged.

References

[1] Michael Batty. *Cities and complexity: understanding cities with cellular automata, agent-based models, and fractals*. MIT Press, Cambridge, Mass., 1. paperback ed edition, 2007. OCLC: 845168184.

[2] A Turing. The chemical basis of morphogenesis. *Bulletin of Mathematical Biology*, 52(1-2):153–197, 1990.

[3] S. Kondo and T. Miura. Reaction-Diffusion Model as a Framework for Understanding Biological Pattern Formation. *Science*, 329(5999):1616–1620, September 2010.

Proceedings of WANCSA 2017
Normandie University, Le Havre, France - July 3-4, 2014

LOCAL NASH EQUILIBRIUM AND UNFAVORABLE INDIVIDUALS IN SOCIAL NETWORKS

Yichao Zhang, Jihong Guan and Shuigeng Zhou *†‡

Abstract. In this talk, we mainly discuss two topics: local Nash equilibrium and unfavorable individuals in social gaming networks.

Nash equilibrium is widely present in various social disputes. As of now, in structured static populations, such as social networks, regular, and random graphs, the discussions on Nash equilibrium are quite limited. In a relatively stable static gaming network, a rational individual has to comprehensively consider all his/her opponents strategies before they adopt a unified strategy. In this scenario, a new strategy equilibrium emerges in the system. We define this equilibrium as a local Nash equilibrium. We present an explicit definition of the local Nash equilibrium for the two-strategy games in structured populations. Based on the definition, we investigate the condition that a system reaches the evolutionary stable state when the individuals play the Prisoners dilemma and snowdrift game. The local Nash equilibrium provides a way to judge whether a gaming structured population reaches the evolutionary stable state on one hand. On the other hand, it can be used to predict whether cooperators can survive in a system long before the system reaches its evolutionary stable state for the Prisoners dilemma game.

In the second topic, we investigate the topological properties of unfavorable individuals in evolutionary games. The unfavorable individuals are defined as the individuals gaining the lowest average payoff in a round of game. Since the average payoff is normally considered as a measure of fitness, the unfavorable individuals are very likely to be eliminated or change their strategy updating rules from a Darwinian perspective. Considering that humans can hardly adopt a unified strategy to play with their neighbors, we propose a divide-and-conquer game model, where individuals can interact with their neighbors in the network with appropriate strategies. We test and compare a series of highly rational strategy updating rules. In the tested scenarios, our analytical and simulation results surprisingly reveal that the less-connected individuals in degree-heterogeneous networks are more likely to become the unfavorable individuals. Our finding suggests that the connectivity of individuals as a social capital fundamentally changes the gaming environment.

Keywords. Game theory, social networks, Nash equilibrium, scale-free networks, small-world networks.

*Yichao Zhang and Jihong Guan are with Department of Computer Science and Technology, Tongji University, China. E-mails: yichaozhang@tongji.edu.cn, jhguan@tongji.edu.cn

†Shuigeng Zhou is with Department of Computer Science and Engineering, Fudan University, China. E-mail: sgzhou@fudan.edu.cn

‡Manuscript received April 19, 2009; revised January 11, 2010.

Proceedings of WANCSA 2017
Normandie University, Le Havre, France - July 4-5, 2017

INFLUENCE OF COUPLING ON EQUILIBRIA AND HOPF BIFURCATIONS IN A NETWORK OF HINDMARSH-ROSE NEURONS

N. Corson, V. Lanza and N. Verdière *

Abstract. In this work, we focus on networks composed of coupled Hindmarsh-Rose (HR) neuron models. One HR neuron admits up to three equilibrium points and can undergo a Hopf bifurcation, with the small parameter corresponding to the ratio of time scales between the fast and the slow dynamics as bifurcation parameter. The studied networks describe a population of neurons interconnected by electrochemical interconnections, called synapses. To understand how the interactions among the neurons influence the appearance and the properties of such global oscillations may be crucial in order to characterize these complex dynamics. From a mathematical point of view, the emergence of coordinated behavior corresponds to the existence of global periodic oscillations, that can arise for example through Hopf bifurcations. Here, we consider directed acyclic networks of bistable units and we investigate the coupling effects on the Hopf bifurcations occurrence and on the number of equilibria of the entire network. Indeed, it is well-known in literature that in case of multistability in a single element of the network, new equilibrium configurations arise due to the coupling.
Keywords. Hindmarsh-Rose system - Hopf bifurcation - bistability - directed acyclic networks - coupling

The main part of this work has been published in [2].

The Hindmarsh-Rose model is an autonomous system of three nonlinear ordinary differential equations able to reproduce the rich dynamics of a neuron, such as spiking, bursting and chaotic behaviors [9]:

$$\begin{cases} \dot{x} &= y + ax^2 - x^3 - z + I \\ \dot{y} &= 1 - dx^2 - y \\ \dot{z} &= \epsilon(b(x - c_x) - z). \end{cases} \tag{1}$$

Parameters a, b and d are experimentally determined, I corresponds to the applied current, while c_x is the x-coordinate of the leftmost equilibrium of the two-dimensional system given by the first two equations of (1) when $I = 0$ and $z = 0$, respectively. As observed in various biological systems, neuron activity presents different time scales. This can be explicitly observed in HR system, in which the first two equations control the fast dynamics while the third one controls the slow one. Therefore, HR neuron model is a slow-fast system and the parameter ϵ corresponds to the ratio of time scales between the slow and the fast dynamics.

In literature, bifurcations analysis in HR neurons have been carried out essentially from a numerical point of view [3, 5, 11, 6], due to the complexity of the theoretical analysis. At our knowledge, few theoretical works have been proposed on Hopf bifurcation in a single HR model (see [1]). In this work, we prove theoretically the existence of Hopf bifurcations and give simpler conditions than in [1] on system parameters for these bifurcations to occur. By exploiting the Hassard method [8], explicit formula are obtained for studying their direction, stability and period.

Furthermore, we focus on Hopf bifurcations in directed acyclic networks of non-identical linearly coupled HR neurons. This type of networks includes different kinds of classical topologies and suitably models the inherent hierarchical structures in the brain [4]. In general, neurons are interacting through synapses [7], which can be either electrical (gap junctions), modeled by linear coupling functions, or chemical (neurotransmitters), modeled by nonlinear coupling functions. Here we suppose to have only electrical synapses and more generally, we consider directed acyclic networks of linearly coupled HR neurons:

$$\begin{cases} \dot{X_1} &= F_1(X_1) \\ \dot{X_2} &= F_2(X_2) + G_2(X) \\ &\vdots \\ \dot{X_N} &= F_N(X_N) + G_N(X), \end{cases} \tag{2}$$

where $X_i : \mathbb{R} \to \mathbb{R}^3$, $X_i = (x_i, y_i, z_i)^T$, $X = (X_1, \ldots, X_N)^T$ and $F_i : \mathbb{R}^3 \to \mathbb{R}^3$,

$$F_i(X_i) = \begin{pmatrix} y_i + ax_i^2 - x_i^3 - z_i + I \\ 1 - dx_i^2 - y_i \\ \epsilon_i(b(x_i - c_x) - z_i) \end{pmatrix}, i = 1, \ldots, N,$$

*N. Corson, V. Lanza and N. Verdière are with Normandie Univ, France; ULH, LMAH, F-76600 Le Havre; FR CNRS 3335, ISCN, 25 rue Philippe Lebon 76600 Le Havre, France. E-mails: nathalie.corson@univ-lehavre.fr, valentina.lanza@univ-lehavre.fr, nathalie.verdiere@univ-lehavre.fr

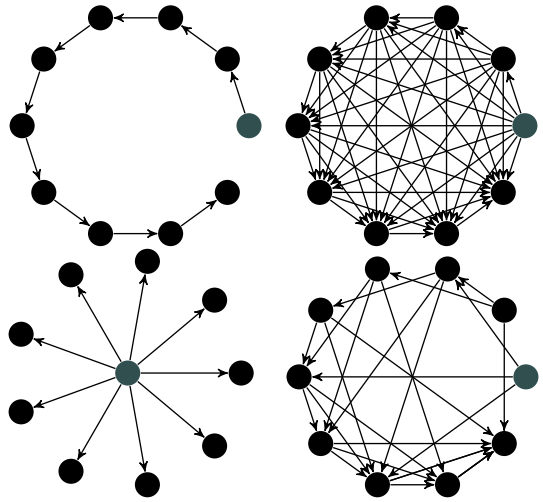

Figure 1: Few examples of directed acyclic networks: chain network (if $k_{ij} = 0\ \forall j \neq i-1$); transitive closure of the chain (and any intermediate state of this closure); star network (if $k_{ij} = 0\ \forall j \neq 1$); any acyclic directed graph with a source vertex.

$$\text{and} \quad G_i(X) = \begin{pmatrix} -\sum_{j=1}^{i-1} k_{ji}(x_i - x_j) \\ 0 \\ 0 \end{pmatrix}, i = 2, \ldots, N.$$

In (2), G_i denotes the linear coupling function between neuron i and the $(i-1)$ first neurons. Moreover, since the coefficients ϵ_i can be different, we consider a directed acyclic network of linearly coupled non-identical HR neurons. This choice of network topology includes different kinds of classical topologies, provided that there is one source node and no cycles. For example, see Fig. 1.

We show how the existence, stability, direction and period of Hopf bifurcations in a directed acyclic network can be theoretically deduced from the analytical results obtained for one neuron. Moreover, the influence of coupling on the existence of Hopf bifurcations and on the appearance (or disappearance) of periodic behaviors is investigated.

Finally, we consider the case when a single HR neuron is bistable and we study the emergence of new equilibria in an acyclic directed network with a source vertex of HR neurons. Indeed, it is well known in literature [10] that in case of multistability we have new equilibrium configurations that arise due to the coupling. It is possible to show that a network of N neurons exhibits up to 3^N equilibria and, by increasing the coupling strength, some of them collide and disappear and, at the end, only trivial equilibria remain. Moreover, the new equilibrium points can undergo Hopf bifurcations.

Acknowledgements

This work is part of the XTerM project, co-financed by the European Union with the European regional development fund (ERDF) and by the Normandie Regional Council.

References

[1] Claudio Buzzi, Jaume Llibre, and João Medrado. Hopf and zero-Hopf bifurcations in the Hindmarsh–Rose system. *Nonlinear Dynamics*, 83(3):1549–1556, 2016.

[2] N Corson, V Lanza, and N Verdière. Hopf bifurcations in directed acyclic networks of linearly coupled Hindmarsh–Rose systems. *Acta biotheoretica*, 64(4):375–402, 2016.

[3] Nathalie Corson and Moulay Aziz-Alaoui. Asymptotic dynamics of Hindmarsh-Rose neuronal system. *Dynamics of Continuous, Discrete and Impulsive Systemes, Series B: Applications and Algorithms*, (16):p–535, 2009.

[4] Jonathan J Crofts and Desmond J Higham. Googling the brain: Discovering hierarchical and asymmetric network structures, with applications in neuroscience. *Internet Mathematics*, 7(4):233–254, 2011.

[5] Enno de Lange. Neuron models of the generic bifurcation type: network analysis. *Thesis, EPFL*, 2006.

[6] JM González-Miranda. Complex bifurcation structures in the Hindmarsh–Rose neuron model. *International Journal of Bifurcation and Chaos*, 17(09):3071–3083, 2007.

[7] Hermann Haken. *Brain Dynamics, An Introduction to Models and Simulations*. Springer-Verlag Berlin Heidelberg, 2008.

[8] Brian D Hassard, Nicholas D Kazarinoff, and Yieh Hei Wan. *Theory and applications of Hopf bifurcation*. Cambridge University Press, Cambridge, 1981.

[9] JL Hindmarsh and RM Rose. A model of neuronal bursting using three coupled first order differential equations. *Proceedings of the Royal Society of London B: Biological Sciences*, 221(1222):87–102, 1984.

[10] RS MacKay and J-A Sepulchre. Multistability in networks of weakly coupled bistable units. *Physica D: Nonlinear Phenomena*, 82(3):243–254, 1995.

[11] Marco Storace, Daniele Linaro, and Enno de Lange. The Hindmarsh–Rose neuron model: bifurcation analysis and piecewise-linear approximations. *Chaos: An Interdisciplinary Journal of Nonlinear Science*, 18(3):033128, 2008.

Proceedings of WANCSA 2017
Normandie University, Le Havre, France - July 4-5, 2017

A MULTI-SCALE NETWORK OF DYNAMICAL SYSTEMS COUPLED BY AGENTS

A. Banos, N. Corson, B. Gaudou and S. Rey-Coyrehourcq *†‡§¶

Abstract. This talk adresses the spread of a disease within a network of interconnected cities. A first possible approach, at a macroscopic scale, consists in coupling ODE systems exploiting populations on nodes and flows on edges (meta-population model). A second approach consists in coupling ODE systems on nodes and agents traveling on edges, making the model hybrid. Under homogegenous conditions, the comparison between the two models leads to similar results on the outputs. However, when it comes to setting up different epidemic control strategies, results rapidly diverge between the two approaches. In this work, we focus on some control strategies, which are quarantine, avoidance and risk culture, to explore the differences, advantages and disadvantages of the two models and discuss the importance of being hybrid when modeling and simulating epidemic spread at the level of a whole urban system.

Keywords. agent-based modeling; city systems; disease spread; mobility; model coupling; metapopulation; network; ODE.

This presentation deals with a work mainly presented in [3]. This work adresses the propagation of an epidemy within interconnected cities interacting through the air network. In each city, an SIR model [10] represents the epidemic dynamics. Mobility between cities is introduced both in an aggregate (MetaPopulation model) and disaggregated (agents) manner. In both cases, we are therefore dealing with coupled SIR on spatial networks.

Interconnected cities modeling often involves coupling processes at different spatial and temporal scales. Single scalar models, whether completely aggregated at the macroscopic scale or completely disaggregated at the microscopic level, are struggling to reach these goals. The spatial and temporal coherence of coupled models at different scales is therefore an important issue. As such, the modeling of the spread of epidemics in structured populations is a particularly active area of application.We focus more specifically on the spread of infectious diseases between cities via air network. The aim is to compare two different formalizations of the same problem: one, described as "MetaPopulation", is based on an aggregate deterministic modeling of coupled urban epidemic dynamics while the other is stochastic and combines aggregated and agent-based modeling.

The first approach - MetaPopulation - comes from researches led in ecology [8, 9] then was applied to various fields, especially in models examining the spread of diseases within networks [2, 11, 4]. This formalism allows handling very large populations being spatially distributed. Corresponding models are mainly used to study the conditions for spread of disease and to test different control strategies or behavioral adaptations at a macro scale [11].

The second approach aims to overcome the limitations inherent to the first one, including heterogeneous populations and behaviors, and is arguably more adapted when it comes to integrate intentionality, reflexivity and adaptability of humans in the model [5, 7, 6].

To our knowledge, only a few works [1] mobilize and compare these two approaches. Papers focusing on agent-based models insist more on the comparison between individual-based models and equation-based models (eg to estimate the parameters of the equations from dynamic generated by individuals interactions [12, 6]).

However, when studying social phenomena, as in a urban context, such couplings may be required. This is the case, for example, once a background dynamics must be introduced forming the evolving context in which individuals or groups of individuals interact. Handling spatial and temporal coherence of the models at different scales is an important issue, as well as the exploration of the properties of hybrid models [11]. Indeed, model coupling brings out a number of fundamental problems, such as:

1. the preservation of population during transfers between the macro scale (rational numbers) and micro scale (whole numbers);

2. the inclusion of a population considered as homogeneous in the aggregated model components and of heterogeneous individuals in its disaggregated components;

*A. Banos is with Geographie-Cits, Paris, France. E-mail: arnaud.banos@parisgeo.cnrs.fr
†N. Corson is with LMAH, Le Havre, France. E-mail: nathalie.corson@univ-lehavre.fr
‡B. Gaudou, is with IRIT, Toulouse, France. E-mails: benoit.gaudou@ut-capitole.fr
§Rey-Coyrehourcq is with IDEES, Rouen, France. E-mails: sebastien.rey-coyrehourcq@univ-rouen.fr
¶Manuscript received June 11, 2017.

3. the articulation of different scales of time and space, handling for example the spread of an epidemic at a city level and the travelling behavior of individuals;

4. the characterization of the behavior of the global model and its properties, which can not be reduced to the properties of each of its components.

In this presentation, we first introduce the two epidemic spread models in a spatial network and then propose a comparison between the two modeling approaches. Mitigation strategies are then introduced at different scales.

Acknowledgements

This work was founded by CNRS (PEPS HuMain 2013 and 2014) and by the French National Network of Complex Systems (RNSC), via the interdisciplinary network MAPS (http://maps.hypotheses.org/).

References

[1] Ajelli, M.; GonCalves, B.; Balcan, D.; Colizza, V.; Hu, H.; Ramasco, J.J. ;Merler, S. ; and Vespignani, A. Comparing wide-scale computational modeling Approaches to epidemic: agent-based versus structured MetaPopulation models. BMC Infectious Diseases, **2010**, 10 (190).

[2] Arino, J. ; Van den Driessche, P.. A multi-city epidemic model. Mathematical Population Studies **2003**, 10 (3): 175-193.

[3] Banos A.; Corson N.; Gaudou B.; Laperrire V.; Rey Coyrehourcq S.; The Importance of Being Hybrid for Spatial Epidemic Models:A Multi-Scale Approach, Systems **2015**, 3(4), pp. 309-329.

[4] Colizza, V. ; Vespignani, A. Epidemic in MetaPopulation modeling systems with heterogeneous coupling pattern: theory and simulations. Journal of Theoretical Biology **2008**, 251: 450-467.

[5] Durrett, R. ; Levin, S. The importance of being white discrete (and spatial). Theoretical Population Biology **1994**, 46 (32): 363-394.

[6] Fahse, L. ; Wissel, C. ; Grimm, V. Reconciling classical and IB Approaches in theoretical population ecology: a protocol for extracting population parameters from IBM. American Naturalist **1998**, 152: 838-852.

[7] Frontier, S. ; Pichod-Viale, D. Ecosystèmes, Structure, fonctionnement, Evolution. Masson, Paris, France, **1990**.

[8] Hanski, I. ; Gilpin, M.E., MetaPopulation Biology: Ecology, Genetics, and Evolution. Academic Press, Waltham, Massachusetts, USA, **1997**.

[9] Levins R. Some demographic and genetic consequences of environmental heterogeneity for biological control. Bull. Entomol. Soc. Am. 15, 237-240, **1969**.

[10] Kermack, W.O. ; McKendrick, A.G. Contributions to the mathematical theory of epidemics. The Journal of Hygiene **1939**, 39 (3): 271-288.

[11] Meloni, S. ; Perra, N. ; Arenas, A. ; Gomez, S. ; Moreno, Y. ; Vespignani, A. Modeling human mobility responses to the wide-scale spreading of infectious diseases. Scientific Reports **2011**, 1, 62(7) : 1-7.

[12] Nguyen, N.D. Coupling Equation-Based and Individual-Based Models in the Study of Complex Systems - A Case Study in Theoretical Population Ecology. PhD thesis, University Pierre and Marie Curie, France, **2010**.

Proceedings of WANCSA 2017
Normandie University, Le Havre, France - July 4-5, 2017

MATHEMATICAL MODELING AND NUMERICAL SIMULATION OF HODGKIN-HUXLEY NEURONS FOR COMPLEX NETWORK IN V1 CORTEX.

Mohamed Maama *

Abstract.

The brain is an interesting machine, our joys, sorrows, memories, and ambitions are no more than the electrical activity of a large assembly of nerve cells.
The brain is the most complex organ in the human body that contains 100 billion of neurons, which have two physiological properties: the excitability, i.e., the ability to respond to stimulations and convert them into nerve impulses, and the conductivity, that means the ability to transmit impulses. Neurons from the same individual are differentiated by changing their genetic, but in the application, we assume that all them are identical.
A neuron consists of dendrites, a cell body, an axon, and synaptic terminals. This structure reflects its functional subdivision into receiving, integrating and transmitting compartments.
It lives in a noisy environment, that is, it is subjected to many sources of noise, for example, the opening and closing of channels is a probabilistic event. Moreover, neurons in the cerebral cortex recorded in vivo show very irregular firing in a large range of firing rates, and there is a wide variability in the spike trains of neurons from trial to trial.
From a dynamical system point of view, neurons are excitable because they are near a transition, called bifurcation, from resting to spiking activity (in the sense that they are typically at rest but can fire spikes).

Or, each neuron is connected to approximately 10000 other neurons. These connections called synapses, are arranged in a highly complex network. They are responsible for neuronal communication and can be classified into two basic mechanisms: chemical synapses and electrical gap junctions.
The electrical synapse is the simplest form of synapse which consists of intercellular channels allowing ions and small molecules to pass from one cell to the next. Clusters of these channels, which consist of proteins, form gap-junctions. Intriguingly, these can be found in almost every mammalian cell. Gap junctions are thought to support to support synchronization of larger populations of neurons (e.g. Hu and Bloomfield, 2003; Perez Velazquez and Carlen, 2000).
Unlike chemical synapses, in electrical synapses the transmission of information from one neuron to another is directly performed from the pre-synaptic cell to the post-synaptic cell via gap junctions.

In chemical synapses, the process occurs via neurotransmitters, which cross the synaptic cleft and bind to receptors on the membrane of the synaptic cell. Neurotransmitters may increase or decrease the probability of an action potential of a post-synaptic neuron, and the synapses are called excitatory or inhibitory, respectively. Furthermore, the intensity of the chemical synapses can be modified, it means that, they can be minimized or potentiated (Dagostin AA, Mello CV, Leao RM. Increased bursting glutamatergic neurotransmission in an auditory forebrain area of the zebra finch (Taenopygia guttata) induced by auditory stimulation).

The electrical current which results from the release of a unit amount of neurotransmitter at the time t_0 is:

$$I_{syn}(t) = g_{syn}(t)(V(t) - E_{syn}), \quad t \geq t_0$$

Where:

- $g_{syn}(t)$ is the synaptic conductance;
- $V(t)$ is the tension across the post-synaptic membrane;
- E_{syn} is the equilibrium potential of the ion channels that mediate the synaptic current.

We consider here the more physiologically realistic Hodgkin-Huxley model. It was developed half a century ago by Alan Hodgkin and Andrew Huxley. They carried out an elegant series of electrophysiological experiments on the squid giant axon in the late 1940s and early 1950s.
The squid giant axon is notable for its extraordinarily large diameter ($0.5mm$). Most axons in the squid nervous system and in other nervous systems are typically at least 100 times thinner.
The large size of the squid giant axon is a specialization for rapid conduction of action potentials that trigger the contraction of the squids mantle when escaping from a predator.
In addition to being beneficial for the squid, the large diameter of the giant axon was beneficial for Hodgkin and Huxley because it permitted manipulations that were not technically feasible in smaller axons that had been used in biophysical studies up to that point. In a well designed series of experiments, Hodgkin and Huxley systematically demonstrated how the macroscopic ionic currents in the squid giant axon could be understood in terms of changes in Na^+ and K^+ conductances in the axon membrane. Based on a series of voltage-clamp experiments, they developed a detailed mathematical model of the voltage-dependent and time dependent properties of the Na^+ and K^+ conductances.

The HH model is a system of four non linear differential equations:

$$\begin{cases} C_m \frac{dV}{dt} = -g_{Na} m^3 h (V - E_{Na}) - g_K n^4 (V - E_K) - g_L (V - E_L) + I_{ext} \\ \frac{dm}{dt} = \alpha_m(V)(1 - m) - \beta_m(V) m \\ \frac{dh}{dt} = \alpha_h(V)(1 - h) - \beta_h(V) h \\ \frac{dn}{dt} = \alpha_n(V)(1 - n) - \beta_n(V) n \end{cases} \tag{1}$$

Where:

$$\alpha_m(v) := \begin{cases} \frac{0.1(v+40)}{(1-\exp(\frac{-(v+40)}{10})} & v \neq -40, \\ 1 & v = -40. \end{cases}$$

$$\beta_m(v) := 4\exp(\tfrac{-(v+65}{18}).$$

$$\alpha_h(v) := 0.07\exp(\tfrac{-(v+65}{20}).$$

*PhD student in Laboratory of Applied Mathematics, Normandie University, Le Havre, France. E-mail: mohamed.maama@univ-lehavre.fr

$\beta_h(v) := \frac{1}{1+\exp(\frac{-(v+35)}{10})}$.

$\alpha_n(v) := \begin{cases} \frac{0.01(v+55)}{(1-\exp(\frac{-(v+55)}{10})} & v \neq -55, \\ 0.1 & v = -55. \end{cases}$

$\beta_n(v) := 0.125\exp(\frac{-(v+65)}{80})$.

Inversion potentials	Maximum Conductance
$E_K = -77\ mV$	$\overline{g}_K = 36\ mS/cm^2$
$E_{Na} = 50\ mV$	$\overline{g}_{Na} = 120\ mS/cm^2$
$E_L = -54.4\ mV$	$\overline{g}_L = 0.3\ mS/cm^2$

The differential equation corresponding to the synaptic conductance is as following:

$$\tau \frac{dg_{syn}(t)}{dt} = -g_{syn}(t) + \overline{g}_{syn}\delta(t - t_0),$$

Where $\delta(t)$ is a Dirac distribution that takes an infinite value at 0, and the zero value elsewhere, and whose integral over $\mathbb{R}$ is equal to 1. $\delta(t) = \begin{cases} +\infty, & t = 0 \\ 0, & t \neq 0 \end{cases}$ et $\int_{-\infty}^{+\infty} \delta(t)\, dt = 1$.

Also $\delta_a(t) = \lim_{a \to 0} \frac{1}{a\sqrt{2\pi}} e^{\frac{-t^2}{2a^2}}$,

The primary visual area (V1) of the cerebral cortex is the first stage of cortical processing of visual information. Area V1 contains a complete map of the visual field covered by the eyes. It receives its main visual input from the lateral geniculate nucleus of the thalamus (LGN), and sends its main output to subsequent cortical visual areas (Maunsell and Newsome, 1987; Van Essen and Felleman, 1991).

Thanks to high neuronal density and large area, V1 contains a vast number of neurons. In humans, it contains about 140 million neurons per hemisphere (Wandell, 1995), i.e. about 40 V1 neurons per LGN neuron. Such divergence gives scope for extensive processing of the images received from LGN.
The visual input to the brain begins in the retina that is able to convert light from different parts of visual stage into a code. This code is composed of electrical impulses called spikes or action potentials. After that it goes to LGN and then to primary visual cortex V1 that located at the back of the head.

V1 is one of the best understood areas of the cerebral cortex, and constitutes a prime workbench for the study of cortical circuits and of computations. Numerous factors contribute to this fortunate position: we understand the nature of its main inputs, we know what stimuli make its neurons fire, and we can easily make those stimuli thanks to computer displays. Moreover, in many species area V1 lies at least partly on the surface, and is therefore particularly accessible for various imaging methods.

The mammalian primary visual cortex (V1) plays an integral role in many discrimination, recognition and classification tasks. It performs diverse functions, and is well known to be immensely complex. As a dynamical system, V1 likely demands many degrees of freedom to support the great variety of dynamical processes accompanying its many visual tasks. The aim of the present study is to gain insight into these processes via computational modeling: We designed a mechanistic model, carefully benchmarked it using physiological data, and analyzed the underlying dynamics.

In this work, we introduce a complex network dynamics of Hodgkin-Huxley (HH) neurons with chemical synapses to model a local neuronal population in V1 as following:

$$\begin{cases} C_m \frac{dV}{dt} = -g_{Na} m^3 h (V - E_{Na}) - g_K n^4 (V - E_K) - g_L (V - E_L) \\ \qquad\qquad -g_E (V - V_E) - g_I (V - V_I) + I_{ext} \\ \frac{dm}{dt} = \alpha_m(V)(1 - m) - \beta_m(V) m \\ \frac{dh}{dt} = \alpha_h(V)(1 - h) - \beta_h(V) h \\ \frac{dn}{dt} = \alpha_n(V)(1 - n) - \beta_n(V) n \end{cases} \tag{2}$$

For a neuron n of type $Q \in \{E,\ I\}$, its conductances satisfy the following equations:

$$\begin{cases} \tau_E \frac{dg_E}{dt} = -g_E + S^{QE} \sum_{i=1}^{\infty} \delta(t - t_i^{syn,E}) + S^{dr} \sum_{i=1}^{\infty} \delta(t - t_i^{dr}) \\ \tau_I \frac{dg_I}{dt} = -g_I + S^{QI} \sum_{i=1}^{\infty} \delta(t - t_i^{syn,I}) \end{cases} \tag{3}$$

And we focus on the numerical simulation of all-to-all coupled HH networks with Poisson spike inputs. In this talk, I will start by an overview of V1 cortex, the physiology of neurons and chemical synapses, after that I will show our model associated to V1 and its numerical results.

Acknowledgements

This work is part of the XTerM project, co-financed by the European Union with the European regional development fund (ERDF) and by the Normandie Regional Council.

References

[1] L. F. Abbott, D. Peter, *Theoretical neuroscience*, Cambridge, MA: MIT Press, vol. 806, 2001.

[2] W. Gerstner, W. M. Kistler, R. Naud, and L. Paninski, *Neuronal dynamics: From single neurons to networks and models of cognition*, Cambridge University Press, 2014.

[3] A. Hodgkin, A. Huxley, "Propagation of electrical signals along giant nerve fibres," *Proceedings of the Royal Society of London. Series B, Biological Sciences*, pp.177–183, 1952.

[4] B. Hassard, "Bifurcation of periodic solutions of the Hodgkin-Huxley model for the squid giant axon," *Journal of Theoretical Biology.*, vol. 71, pp. 401-420, 1978.

[5] GB. Ermentrout, DH. Terman, "Mathematical foundations of neuroscience", *Springer*. vol. 35, 2010.

[6] L. Chariker, LS. Young, "Emergent spike patterns in neuronal populations", *Journal of computational neuroscience*, vol. 38, pp. 203-220, 2015.

[7] L. Chariker, R. Shapley, LS. Young, "Orientation Selectivity from Very Sparse LGN Inputs in a Comprehensive Model of Macaque V1 Cortex", *Journal of Neuroscience*, vol. 36, pp.12368–12384, 2016.

Proceedings of WANCSA 2017
Normandie University, Le Havre, France – July 4-5, 2017

Generalized synchronization and system parameters identification between two different complex networks

Xiang Wei, Junchan Zhao, and Chunhua Hu

Abstract. This paper proposed a method to identify system unknown parameters of complex network. Aim at system unknown parameters, a method which used generalized synchronization (GS) was proposed. This method base on the Barbalat lemma and Lyapunov stability scheme, an auxiliary complex network with different topology and different dynamics is constructed, and some adaptive controllers are designed to identify system parameters upon GS with delay coupling. Compare to the method based on complete outer synchronization, the proposed method can construct the simple and low dimensions dynamics to identify the parameters of high dimensions dynamics. Numerical simulations are provided to show the effectiveness of the proposed method.
Keywords. Complex networks, Generalized synchronization, Parameters identification, Adaptive controller

1 Introduction

Complex networks, such as transportation and phone networks, the Internet, wireless networks, and the World Wide Web, play an important role in our life. Significant progress has been made in understanding complex networks since the discovery of their small-world [1] and scale-free [2] characteristics. Recently, synchronization of complex networks has evoked broad interest. Two basic tools are used to analyze various synchronization problems encountered in complex networks. The first is the master stability function, proposed by Pecora and Carroll [3], and the other is the connection graph stability method, proposed by Belykh et al. [4,5].

However, many complex network synchronization studies assume that system parameters are known. When the system parameters are unknown, it is difficult to study complex network synchronization. For complex networks with unknown system parameters, we first set it as a drive network, and then construct a respond network with different structure and dynamical equations. The generalized synchronization of a coupled delay network is realized and the parameters of the system are successfully identified.

1. Xiang Wei is with Department of Engineering, Honghe University, Honghe Yunnan 661100
2. Junchan Zhao is with School of Mathematics and Statistics, Hunan University of Commerce, Changsha Hunan 410205
3. Chunhua Hu is with Key Laboratory of Hunan Province for Mobile Business Intelligence, Hunan University of Commerce, Changsha Hunan 410205.

2 Drive and response network model

Consider the following a drive and response network model, and the system parameters of the drive network are unknown. Each network contains N nodes, and the dynamic in each network is same. However, the structure of each network is different. The upper layer is the driving network, and the lower layer is response network, as shown in Figure 1.

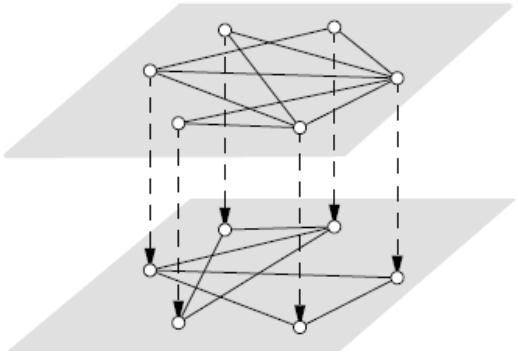

Fig. 1 Model of drive network and response network(dashed
links as interlayer links between networks)

The network model is described as below

$$\dot{\boldsymbol{x}}_i(t) = \boldsymbol{f}(x_i(t))) + w_1 \sum_{j=1}^{N} c_{ij}\Gamma_1 \boldsymbol{x}_j(t-\tau), \quad i = 1, 2, ..., N; \qquad (1)$$

$$\dot{\boldsymbol{y}}_i(t) = \boldsymbol{g}(\boldsymbol{y}_i(t)) + w_2 \sum_{j=1}^{N} d_{ij}\Gamma_2 \boldsymbol{y}_j(t-\tau) + \boldsymbol{u}_i(t), \quad i = 1, 2, ..., N. \qquad (2)$$

Where *x* and *y* are the dynamic states of the drive and response systems, respectively. The functions *f* and *g* are node dynamics of the drive and response systems. *c* is the coupling matrix, and use *d* to estimate the topology of the drive network.

The drive and the response network is generalized synchronization if

$$\lim_{t\to\infty} \| \boldsymbol{y}_i(t) - \boldsymbol{\Phi}_i(\boldsymbol{x}_i(t)) \| = 0, \quad i = 1, 2, ..., N. \qquad (3)$$

3 Main results

In this section, the generalized synchronization and parameters identification are studied.
First, define the synchronization error

$$\boldsymbol{e}_i = \boldsymbol{y}_i(t) - \boldsymbol{\Phi}_i(\boldsymbol{x}_i(t)).$$

Then, set the controller and the adaptive function

$$\begin{aligned}\boldsymbol{u}_i &= \boldsymbol{J}_{\boldsymbol{\Phi}_i}\bar{\boldsymbol{f}}(\boldsymbol{x}_i(t)) + \boldsymbol{J}_{\boldsymbol{\Phi}_i}\bar{\boldsymbol{F}}(\boldsymbol{x}_i(t))\hat{\boldsymbol{\alpha}} \\ &+ \boldsymbol{J}_{\boldsymbol{\Phi}_i} w_1 \sum_{j=1}^{N} c_{ij}\Gamma_1 \boldsymbol{x}_j(t-\tau) - \boldsymbol{g}(\Phi_i(\boldsymbol{x}_i(t))) \\ &- w_2 \sum_{j=1}^{N} d_{ij}\Gamma_2 \phi_j(\boldsymbol{x}_j(t-\tau)) - k_i \boldsymbol{e}_i(t),\end{aligned}$$

$$\dot{\hat{\boldsymbol{\alpha}}} = -\sum_{i=1}^{N} \bar{\boldsymbol{F}}_i^{\mathsf{T}}(\boldsymbol{x}_i(t))\boldsymbol{J}_{\boldsymbol{\Phi}_i}^{\mathsf{T}}(\boldsymbol{x}_i(t))\boldsymbol{e}_i(t),$$

$$\dot{k}_i = \|\boldsymbol{e}_i(t)\|^2,$$

Then, under the controllers and adaptive regular, the drive and response network can reach generalized synchronization, and the system parameters of the drive network can be identified.

Acknowledgment

The research for this work was supported by National Natural Science Foundation of China (61174028, 41301442, 61273232), The Program for New Century Excellent Talents in University(NCET-13-0785).

References

[1] Watts D J, Strogatz S H. Collective dynamics of 'small-world' networks. Nature, 1998, 393: 440– 442.
[2] Barabasi A L, Albert R. Emergence of scaling in random networks. Science, 1999, 286(5439): 509–512.
[3] Pecora L M, Carroll T L. Master stability function for synchronized coupled systems. Phys Rev Lett, 1998, 80: 2109–2112.
[4] Belykh V N, Belykh I V, Hasler M. Connection graph stability method for synchronized coupled chaotic systems. Phys D, 2004, 195: 159–187
[5] Belykh I V, Belykh V N, Hasler M. Generalized connection graph method for synchronization in asymmetrical networks. Phys D, 2006, 224: 42–51

Proceedings of WANCSA 2017
Normandie University, Le Havre, France - July 3-4, 2017

A CASCADING FAILURE MODEL TO STUDY STRESS PROPAGATION IN CROWDS

Rodolphe Charrier *†

Abstract. This work proposes an enhancement of the classical Helbing's model of crowd dynamics with a nervosity factor, by adding an emotional propagation network within the crowd seen as a social network.

Keywords. Crowd dynamics, complex networks, emotional contagion, panic disorders, Coupled map networks

1 Introduction

Emotional propagation in crowds is a key problem when one intends to understand and model crowd phenomena in critical situations, like the panic emergence during catastrophic events and emergency situations. One may think about many recent events link with earth quakes, terrorism attacks and so on ... Our approach here is indeed based on the postulate that emotions, namely strong emotions, can propagate within the crowd, sometimes very rapidly. This approach fits the theory of emotional contagion, mainly adopted among north american psychologists [1], which is based on mimicry behaviors through perceptions. However, this study is made difficult by the lack of real data, or at least of sufficiently exploitable data. One of the other difficulties is the fact that these sort of phenomena can not easily be reproduced by experiment, because of legal and ethical reasons. That is why one of the most convenient way to tackle the problem is computer simulation using basic models. One of the most famous model, the one we use here, is the Helbing's social force model [2] based on a particle system modeling. In details, this model describes the kinematics of a multi-agent system behaving like solid balls. An evolution of this model have been proposed to deal with panic situation by including a nervosity factor in [3]. But this nervosity keeps beeing only a kinematic quantity which depends only on the velocity of individuals, and therefore can not really account for the nervosity contagion observed by psychologists.

Our approach gives an internal and network dimension to the nervosity factor of Helbing's model to fill this gap. The network dimension is revealed by the network of perception between agents within the crowd, while the internal dimension is linked with a coupled map model. The scenario we study in this work is inspired by some cascading failure problems [4] : an agent/node of the network becomes suddenly highly nervous/stressed. We then observe the outcome of the emotional perturbation within the network, while this perturbation propagates through the directed edges of the network.
To finish with this overview of our modeling approach, a last point is to be mentioned : what is the failure in our problem and how to characterize it? A possible answer is given by medical studies on panic disorders : when panic disorders appear in human beings, it can be revealed by a high chaotic signature (measured by entropy calculus) of internal physiological signals like the heart beat and/or the respiratory frequency [6]. This important point may validate the resort to the specific dynamical model of Coupled Map Network (CMN) [5], which can give chaotic dynamics with linear couplings, to simulate the propagation of the stress/nervosity in the crowd in our simulations.

2 Modeling design

The Helbing's model of social forces with nervosity may be written in two parts in the the main dynamic law (we won't go into details here, details can be found for example in the paper [3]):

$$m_i \frac{d\mathbf{v_i}(t)}{dt} = \gamma_\mathbf{i}(t) + \xi_\mathbf{i}(t)$$

- the first term is the sum of forces exerted on an agent i (in order: an individual goal/motivation force, repulsive social forces, contact social forces and repulsive forces to avoid obstacles) which is written:

$$\gamma_\mathbf{i}(t) = \mathbf{g_i}(t) + \mathbf{f_i^{soc}}(t) + \mathbf{f_i^{ph}}(t) + \mathbf{f_i^{obs}}(t)$$

- and the second term is a fluctuation term evolving between two extrem values, which is governed by the nervosity n_i of the agent i:

$$\xi_\mathbf{i}(t) = (1 - n_i)\ \eta_\mathbf{0} + n_i\ \eta_\mathbf{max}$$

*Rodolphe Charrier is with Laboratory of Computer Science, Information Processing and Systems, Le Havre Normandy University, Le Havre. E-mails: Rodolphe.Charrier@univ-lehavre.fr
†Manuscript received June, 2017

the nervosity factor is only given by the ratio between the desired velocity of the agent and his averaged velocity (it is bound in $[0, 1]$):

$$n_i(t) = 1 - \frac{\overline{v}_i(t)}{v_i^0}$$

Our approach intends to couple this nervosity factor with another internal parameter x_i of the agent i bound in $[0, 1]$, which gives the emotional dynamics of the agent depending on the interaction network where he evolves. The interaction network is determined by the relative perceptions between agents (see fig. 1). On this network, the parameter is governed by the master updating equation (the same as Coupled Map Networks):

$$x_i(t+1) = (1-\epsilon)f(x_i(t)) + \frac{\epsilon}{|V_i|}\sum_{j\in V_i} f(x_j(t))$$

where f is the nonlinear logistic map :
$f(x_i(t)) = 4\, a_i\, x_i(t)(1-x_i(t))$ with the control parameter a_i: when $a_i = 1$, this map generates chaotic time series, which can be detected by calculating the entropy S_i of the series. If $S_i > 0$ then the series is chaotic [7]. The linear coupling leads to propagate the chaotic dynamic within the network.
The last aspect is the link between the nervous factor and the emotional dynamic parameter x_i by the two following formula:

$$a_i(t) = (1 - n_i(t))a_i(0) + n_i(t)$$
$$n_i(t) = F((1 - \frac{\overline{v}_i(t)}{v_i(0)}) * (\frac{2}{1+\exp^{-S_i(t)}})$$

where $F(z) = min\{z, 1\}$ and $S_i(t)$ is the entropy calculated on the x_i time series.
Doing this, we get a feedback loop between the movement of the crowd and the emotional propagation network.

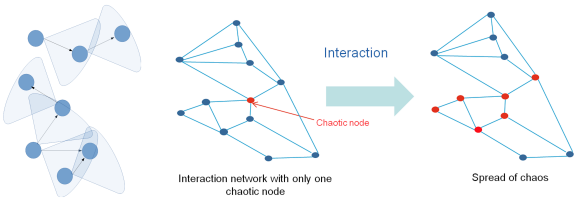

Figure 1: Construction of the perception network and propagation of a chaotic signal in the network [8].

Our scenario of cascading failure is as follows: to begin with we consider failure in our problem as the chaotic signature of a dynamic signal, linking with medical observation (cf. introduction). Then when a first agent becomes highly nervous/stressed, that is his emotional internal parameter x_i becomes chaotic (revealed by the entropy $S_i > 0$), he begins to transmit his nervousness to others in the crowd by perceptive interaction/coupling. Then many agents can get nervous/stressed without seeing any immediate danger.

3 Simulations and Main results

We show in this section some results of simulations using the preceding model in a corridor with a bottleneck caused by obstacles (fig.2).

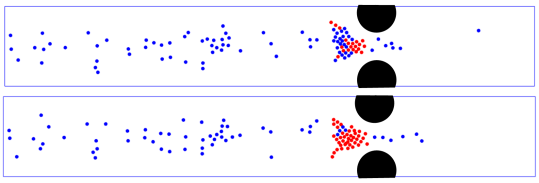

Figure 2: Simulations of stress propagation from top to bottom with the Helbing's model and with our propagation network at the same time step. "Normal" agents are in blue while nervous agents are in red [8].

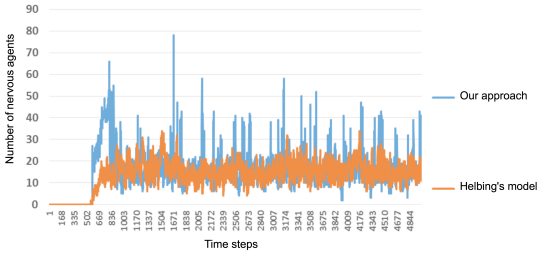

Figure 3: Comparison of the number of nervous agents (agents with a nervosity factor over 0.5) [8].

The main outcome lies in the fact that stress propagation makes the agents very nervous very soon, that is the information of a problem propagates very fast in the system, upstream to the obstacle (see fig.3). Moreover this information produces a counterintuitive effect here, that is a better fluidity of the crowd.

Acknowledgements

This work is part of the XTerM project, co-financed by the European Union with the European regional development fund (ERDF) and by the Normandie Regional Council.
This research was also supported by the french Ministry of Higher Education and Research with the funding of the PhD [8].
Special thanks to Cyrille Bertelle, professor at Le Havre Normandy University for his supervising.

References

[1] E. Hatfield,J. T. Cacioppo,R. L. Rapson, "Emotional Contagion",*Studies in emotion and social interaction*, Cambridge University Press, 1994.

[2] D. Helbing,P. Molnar,"Social force model for pedestrian dynamics",*Physical Review E*, vol. 51, pp.4282-4286, 1995.

[3] D. Helbing, I. Farkas, T. Vicsek, "Simulating dynamical features of escape panic," *Nature*, vol. 407, pp.487-490, 2000.

[4] J Xu, X. F.Wang, "Cascading failures in scale-free coupled map lattices," *Physica A*, vol. 349, pp. 685-692, 2005.

[5] K. Kaneko, "Clustering, coding, switching, hierarchical ordering, and control in a network of chaotic elements" *Physica D*, vol. 41, pp. 137-172, 1990.

[6] D. Caldirola,L. Bellodi,A. Caumo,G. Migliarese,G. Perna, "Approximate entropy of respiratory patterns in panic disorder",*Am J Psychiatry*, vol. 161, pp.79-87, 2004.

[7] N. Marwan, M. C. Romano,M. Thiel,J. Kurths, "Recurrence plots for the analysis of complex systems",*Physics Reports*,vol. 438, pp.237-329.,2007.

[8] H. Rabai, *Réseau dynamique d'applications chaotiques couplées pour l'étude de la mobilité urbaine*, PhD Thesis, Le Havre Normandy University, december 2016.

Proceedings of WANCSA 2017
Normandie University, Le Havre, France - July 3-4, 2014

IDENTIFICATION OF A SOURCE ON A NETWORK

Jean-Guy CAPUTO, Adel Hamdi and Arnaud KNIPPEL

[1]

Keywords. miscible flows on networks, source detection, Laplacian matrix, spectral graph theory

Abstract

We study how to identify a time-dependent source on a node for a wave equation on a network. We prove, under reasonable assumptions, that the time records of two strategic nodes yield uniqueness of the source node and source signal. We develop a non-iterative identification method to localize the source node. The source signal is then calculated using two expressions based respectively on a convolution and a Fourier expansion. Numerical results on a simple graph confirm the soundness of the approach and show that it can be easily implemented in practice.

Acknowledgements

This work is part of project XTerM, funded with the support from the European Union with the European Regional Development Fund (ERDF) and from the Regional Council of Normandie.

[1] Jean-Guy CAPUTO, Adel Hamdi and Arnaud KNIPPEL are with Laboratoire de Mathématiques, INSA de Rouen,
Normandie Université, 76801 Saint-Etienne du Rouvray, France.
E-mails: caputo@insa-rouen.fr, adel.hamdi@insa-rouen.fr, arnaud.knippel@insa-rouen.fr

Proceedings of WANCSA 2017
Normandie University, Le Havre, France - July 3-4, 2017

USING BLOCKCHAIN TO SECURE TRANSACTIONS FOR LOGISTICS NETWORKS IN SMART PORTS

Narimane Benhellal, Claude Duvallet and Cyrille Bertelle *

Abstract. Logistics networks and decentralized supply chains are main applications of complex networks. New challenges of their evolution through connected intelligent infrastructures need new concepts to fluidify and secure transactions.
In particular, port systems tend to digitization and automation of data based on Smart Port concept in order to improve port services and optimize transport flows. To secure transactions in a Smart Port, we propose to use Blockchain technology by dint of its opportunities in terms of transparency (or traceability), interoperability, secure and decentralized exchanges without the oversight or intermediation of any third party. In this paper, we will present Blockchain technology, its benefits as well as its use for transportation networks in Smart Ports.
Keywords. Smart Port, Blockchain, Distributed Database, Security, Decentralized architecture.

1 Introduction

Intelligent transport represents a new concept of information and communication in the field of transportation. It provides new logistics and transportation applications and supply chain management solutions. It can also optimize the tracking and delivery of goods. The Smart Port concept has attracted the attention of big and medium-sized commercial ports such as the Port of Hamburg, Port of Amsterdam, and Port of Le Havre [1]. The main goal is to collect sensor data and automate process while focusing on IoT (Internet of Things [2]), Big Data and business intelligence technologies.

Smart port extends smart city concept [3] in term of technological integration but also in term of energetic management and environmental issues. The smart concept is applying to territorial transformation in term of port-city interface to improve the previous issues to the benefit of citizen.

In order to make the Smart Port concept an enabler of port strategies, we have to know how to gather data that belongs to different sensor owners (terminals, port authorities, truckers, etc.) and how to manage the exchange of this data safely [4].

*n.benhellal, c.duvallet and c.bertelle are with LITIS, Normandie Univ, France. E-mails: n.benhellal@gmail.com, claude.duvallet@univ-lehavre.fr, cyrille.bertelle@univ-lehavre.fr

The port of the future must respond to many challenges facing the port sector such as speed and size of ships which have an impact on the productivity of the port. To achieve that, the port must be smarter by using innovative technologies to avoid the waste of space, time and resources.

Smart port allows to use the existing capacities of the port optimally and maximally. It allows an efficient use of energy and infrastructure, it minimize energy consumption and achieves highest levels of pollution reduction by using innovative transportation planning [5].

Beyond the Smart Port Concept, a new innovative technology called Blockchain has upsetted the advent of the Internet [6]. Thanks to Blockchain, it becomes possible to exchange data with others without passing through an intermediary trusted third party, with a minimal cost and in a secure way [7].

In the following sections, we will show how to use the Blockchain to secure transactions for transportation networks in Smart Ports. Firstly, a presentation of Blockchain technology as well as its benefits and operating principle will be made. Secondly, we will present the benefits of using Blockchain in Smart Port for logistics networks. Finally, we will emphasize some related perspectives for future research work.

2 Blockchains to secure transaction networks

2.1 Overview

Blockchain consists of digital containers on which are stored information of all kinds: transactions, contracts, payment, works of art, etc. All of these blocks form a digital and decentralized database that stores and transfers data via Internet [8] in a transparent, secure and autonomous way and without a central control [9].

Cryptographic tools are implemented to ensure the safe and secure functioning of the distributed ledger [9]. The Blockchain can authenticate, certify and record data and preserve their integrity.

Validation of transactions in Blockchain is carried out independently and randomly by the members (nodes) of

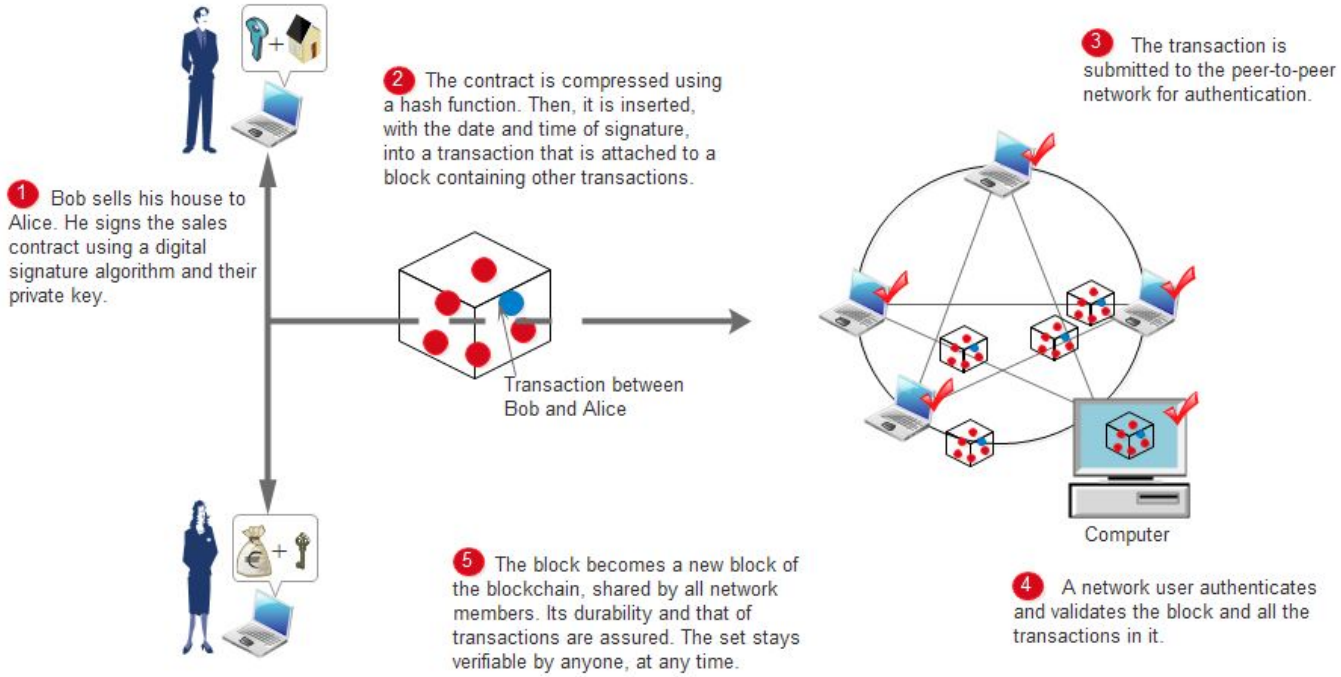

Figure 1: Authenticate the sale of a property through the Blockchain [10].

the peer-to-peer network on which Blockchain is maintained, and that allows exchange and direct sharing of files between computers. This random process makes excessively difficult the premeditated injection of false transactions in Blockchain. The Blockchain therefore allows for a system based on trust, without the need for the parties involved in a transaction to trust each other.

Regarding to security aspect of Blockchain, our idea is to use it and its decentralized architecture in order to facilitate maritime operations since the data and transactions are recorded in blocks and to be able to offer new opportunities to all parties and reduce risks.

2.2 The operating principle

The most known application of Blockchain is Bitcoin. To understand the functioning of this technology, we will explain briefly Bitcoin mechanism.

Bitcoin customers must create a virtual wallet. This one is destined to receive their virtual money. It also contains (at least) a public key, which authenticates the author of each transaction, and a private key, which allows to sign transactions. Finally, we find in this wallet a Bitcoin address which is obtained from the public key by using "hashing" operation, which makes it possible to associate a set of data with a unique "digital print".

If one of the users wants to transfer a block that contains information of several transactions to be validated, the block is then broadcast through all the nodes of the peer-to-peer network which manages the Blockchain Bitcoin (see figure 1).

3 Using Blockchain in Smart Port for Logistics Networks

The possibilities of safely sharing between parties of Blockchain technology create many opportunities for logistics and supply chain applications. It creates a permanent digital public register of transactions that can be shared across a distributed network.

The benefits of Smart Ports include enhancement of transparency and data sharing, reduction of errors and better detection of fraud.

It is also possible to cover a smart contract in Blockchain to eliminate the use of an intermediary in which the parties have confidence by replacing it with program code auditable by all the parties. Smart contract could shorten the contracting chain between the customer and a company for short contracts. It could also certify and simplify the registration of the chain.

Marine Transport International (MTI) uses Blokchain technology to record and store Verified Gross Mass (VGM) data. Instead of a VGM message delivered sequentially to parties within the supply chain, Blockchain platform can provide a decentralized approach to deliver VGM messages [11].

The use of Blockchain technology could therefore support the digitization efforts of the Smart Ports, thanks to its cryptographic process and its decentralized architecture. It also facilitates maritime operations since data and transactions are recorded in blocks.

The aim of using a plateform of Blockchain in port network is to manage and trace all of its containers around

the world reliably and securely. Reducing fraud, transit time and stock caused by this new system should allow to perform considerable economies [12].

Our vision is to use a sustainable Blockchain platform that meets the requirements of maritime transport systems in terms of security and transparency by connecting transport ecosystems into one distributed network.

4 Conclusion

The use of Blockchain's decentralized platform on transportation networks port, in particular the smart port system, will make possible to manage port operations efficiently and faster, secure production processes at a limited cost, while taking into consideration storage space, time, money and the environment

This work shows the benefits of Blockchain in port world. We will continue to develop the Blockchain technology for the Smart Port concept and implement a collaborative decentralized platform that meets the requirements of logistics networks.

References

[1] *Action plan towards the smart port concept in the mediterranean area smart port*, Med Maritime Integrated Projects Smart-Port.

[2] R. Peeters and S. Baeck, *The Internet of Things in transportation - Port of Hamburg case study*, Siapartners, Octobre 2016.

[3] K. Biswas and V. Muthukkumarasamy, *Securing Smart Cities Using Blockchain Technology*, 2016 IEEE 18th International Conference on High Performance Computing and Communications (HPCC/SmartCity/DSS), Sydney, Australia, 2016, pp. 1392-1393.

[4] Miguel, Montesinos, *Smart Port: A System of Systems Approach, Automation and Optimisation*, Available at: `https://www.porttechnology.org/technical_papers/smart_port_a_system_of_systems_approach`

[5] H.R. Abaie, M. Rastegary, *The Emergence of Smart Ports and Their Impactful Implications.*, 24th-25th January 2017. Available at: `http://www.blockchaindailynews.com/Blockchain-et-logistique_a25096.html`

[6] B. Chouli, F. Goujon, Yves-Michel. Leporcher,*Les Blockchains : De la théorie à la pratique de l'idée à l'implémentation*, ENI, jan 2017.

[7] *Blockchain, la technologie qui va bouleverser le monde*, La recherche, N515, sep 2016.

[8] L. Leloup, W. Mougayar , *Blockchain, la révolution de la confiance*, Editions Eyrolles, février 2017.

[9] G. Buffet, *Comprendre la blockchain. Anticiper le potentiel de disruption de la Blockchain sur les organisations*, In : uchange.co, jan. 2016.

[10] C. Cuvelliez, O. Markowitch, J.J. Quisquater. *La machine à créer de la confiance et beaucoup d'espoirs.* Sep 2016.

[11] *Marine Transport International applies blockchain to shipping supply chain* Source: Marine Transport International, September 2016.

[12] *Les premiers pas de la Blockchain dans le domaine maritime*, Mai 2017. Available at: http://news.synchrone-technologies.fr/les-premiers-pas-de-la-blockchain-dans-le-domaine-maritime/

Proceedings of WANCSA 2017
Normandie University, Le Havre, France - July 3-4, 2017

PARAMETER ESTIMATION IN A COUPLED MODEL DESCRIBING THE TRANSMISSION OF THE CHIKUNGUNYA TO THE HUMAN POPULATION.

N. Verdière, S. Zhu and L. Denis-Vidal *†‡

Abstract. This talk adresses a numerical procedure based on a distribution approach for doing parameter estimation in a nonlinear dynamical model describing the transmission of the chikungunya virus to the human population. The advantage of this numerical procedure is not to require any knowledge about the value of the parameters or about the statistics of measurement uncertainties. Furthermore, it attenuates a part of the noise improving consequently the results of the parameter estimation.

Keywords. Parameter estimation, Distribution approach, Nonlinear models, Epidemiological model, Chikungunya virus.

This presentation deals with a submitted work in a journal about the estimation of unknown parameters in a recent model describing the transmission of the chikungunya virus to the human population.
The parameter estimation done from noisy observations can be a difficult and major task for validating a nonlinear model. Parameter estimation is usually carried out by optimizing some criterion function over the parameter space [4, 13]. However, these methods necessitate a first initial guess which can be obtained either by tests in the industrial domain or by a numerical procedure based on measurements [1, 3, 5, 8, 11]. The quality of this first initial guess ensures that the optimization process will take a reasonable amount of time, and may not converge to a local unrealistic solution.

[1, 3, 5, 8, 11] propose each of them a parameter estimation method based on the use of input-output polynomials, that is polynomials depending only on the inputs, the outputs and the parameters of the model. For example, the authors in [8] use iterative integrals in the frequency domain whereas [5] exploits the modulating functions but applied to very simple models. In [3], the authors work in the temporal framework with a distribution approach, this idea being close to the modulating functions.

The advantage of all these methods are that the integral properties permit to decrease the order of derivatives and to incorporate naturally the initial conditions, if necessary. Indeed, their consideration in the numerical estimation procedures may improve the results. As explained in [2, 12], these integrals attenuate the effect of some noises as well.

The chikungunya is a recurrent tropical disease since 50 years. Until 2000, this virus was confined to African countries. However, several epidemics have been reported in non tropical regions as in the Réunion island (a French island in the Indian Ocean) in 2005-2006, in Italy in 2007 or more recently, in the South of America, in the Carabes and in central America in 2014. This epidemic comes from the transmission vector, the Aedes Albopictus [10] that has developed capabilities to adapt to non tropical region.

The authors in [6] developed a model describing the transmission of the chikungunya virus to human population and taken into account the biological life cycle of the mosquito. The difficulty of the model proposed by [6] comes from the different sensitivities of the vector population model to its parameters. Consequently, classical parameter estimation algorithms are difficult to put in place. A first identifiability study had been done on this model in [7, 9]. This study is important in the first step of a parameter estimation procedure since it ensures that the parameter values can be uniquely inferred from input-output measurements. If this property is not verified, the numerical procedure may either fail or give unrealistic parameter values.
In this presentation, we focus our attention on the strategy put in place and based on the distribution method for estimating the parameters of this model.

Acknowledgements

This work is part of the XTerM project, co-financed by the European Union with the European regional development fund (ERDF) and by the Normandie Regional Council.

*N. Verdière is with Normandie Univ, UNIHAVRE, LMAH, FR-CNRS-3335, ISCN, 76600 Le Havre, France. E-mails: nathalie.verdiere@univ-lehavre.fr

†S. Zhu and L. Denis-Vidal are with Applied Mathematics Laboratory of Compiègne (LMAC), University of Technology of Compiègne.

‡Manuscript received June 06, 2017; revised June 06, 2017.

References

[1] F. Boulier, A. Korporal, F. Lemaire, W. Perruquetti, A. Poteaux and R. Ushirobira. An Algorithm for Converting Nonlinear Differential Equations to Integral Equations with an Application to Parameter Estimation from Noisy Data. *Proc. Computer Algebra in Scientific Computing 2014*, number 8660 in LNCS, 28-43, Warsaw, Poland, September (2014).

[2] M. Fliess, M. Mboup, H. Mounier, H. Sira-Ramirez. Questioning some paradigms of signal processing via concret examples, Proc. Summer School: Fast Estimation Method, *Automatic Control and Signal Processing*, Paris (2005).

[3] L. Denis-Vidal, G. Joly-Blanchard, N. Verdière. Identifiability and Estimation of Nonlinear Models: A distribution Framework, *Proc. ECC 2007*, Kos, Grèce, 2-5 juillet (2007).

[4] S. Kiranyaz, T. Ince, M. Gabbouj. Optimization Techniques: An Overview, *Springer Berlin Heidelberg* (2014).

[5] J.M. Loeb, G.M. Cahen, More about process identification, *Automatica*, 359-447 (1965).

[6] D. Moulay, M.A. Aziz-Alaoui, M. Cadivel. The chikungunya disease: Modeling, vector and transmission global dynamics, *Mathematical Biosciences*, 229(1), 50-63 (2011).

[7] D. Moulay, N. Verdière, L. Denis-Vidal. Identifiability of parameters in an epidemiologic model modeling the transmission of the chikungunya, *Proc. MOSIM'2012*, Bordeaux, France, 6-8 june (2012).

[8] H. Sira-Ramrez, C. Garca Rodrguez, J. Cortes Romero, A. Luviano Jurez. Algebraic Identification and Estimation Methods, *Feedback Control Systems*, Wiley (2014).

[9] Z. Shousheng, L. Denis-Vidal, N. Verdière. Identifiability study in a model describing the propagation of the chikungunya to the human population, *Proc. MOSIM'2014*, Nancy, France, 5-7 November (2014).

[10] P. Reiter, D. Fontenille, C. Paupy. Aedes albopictus as an epidemic vector of chikungunya virus: another emerging problem?, *The Lancet Infectious Diseases*, 6(8), 463 - 464 (2006).

[11] N. Verdière, L. Denis-Vidal, G. Joly-Blanchard, D. Domurado. Identifiability and estimation of pharmacokinetic parameters for the ligands of the macrophage mannose receptor, *Int. J. Appl. Math. Comput. Sci.*, 15, 517-526 (2005).

[12] N. Verdière, L. Denis-Vidal, G. Joly-Blanchard. A new method for estimating derivatives based on a distribution approach, *Numerical Algorithm*, 61(1), 163 - 186 (2012).

[13] E. Walter, L. Pronzato. Identification of Parametric Models from Experimental Data, *Springer-Verlag, Berlin* (1997).

Proceedings of WANCSA 2017
Normandie University, Le Havre, France - July 4-5, 2017

PERIODIC ORBITS IN NONLINEAR WAVE EQUATIONS ON NETWORKS

J. G. Caputo*, I. Khames*, A. Knippel* and P. Panayotaros †

Keywords. Graph wave equation, normal modes, nonlinear periodic orbits, ϕ^4 lattice, graph Laplacian.

Abstract

We consider a discrete nonlinear wave equation (discrete ϕ^4 model [1]) in an arbitrary finite graph. The system can be used to model coupled electromechnical oscillators.
We show that inspecting the normal modes of the graph Laplacian [2], we can immediately identify which ones can be extended into nonlinear periodic orbits (generalizing work of Aoki [3]).
We define monovalent, bivalent and trivalent nonlinear periodic orbits depending whether their components are $+1$ or $-1, +1$ or $-1, 0, +1$. Modes without 0 (soft nodes [4]) include the Goldstone [5] and the bivalent modes, solutions with spatial patterns that are typical for systems with power nonlinearity but are absent for the widely studied Fermi-Pasta-Ulam (FPU) systems and lead to different ways for the system to distribute energy.
We perform a systematic linear stability (Floquet) analysis of these orbits. The linearized equations for Goldstone and bivalent orbits are decoupled. For chains (linear graphs), we find that the Goldstone mode is stable for a wide range of parameters while the bivalent mode is always unstable.
The stability analysis for modes with soft nodes is more complicated. Numerical results for trivalent orbits show that periodic orbits that continue nondegenerate linear modes are unstable below an amplitude threshold. Orbits continued from modes with frequency degeneracy are always unstable and we can see the growth of other modes, as indicated by our analysis.

*Laboratoire de Mathmatiques, INSA de Rouen. 76801 Saint-Etienne du Rouvray, France. E-mails: caputo@insa-rouen.fr, imene.khames@insa-rouen.fr, arnaud.knippel@insa-rouen.fr .

†Depto. Matemáticas y Mecánica, IIMAS-UNAM, Apdo. Postal 20-126, 01000 México DF, México. E-mail: panos@mym.iimas.unam.mx .

Acknowledgements

This work is part of the XTerM project, co-financed by the European Union with the European regional development fund (ERDF) and by the Normandie Regional Council. We gratefully acknowledge the financial support from Ecos Nord M15M01.

References

[1] A. C. Scott, *Nonlinear Science: Emergence and Dynamics of Coherent Structures*. Oxford Texts in Applied and Engineering Mathematics (1999).

[2] D. Cvetkovic, P. Rowlinson and S. Simic, *An Introduction to the Theory of Graph Spectra*. London Mathematical Society Student Texts (No. 75) (2001).

[3] K. Aoki, *Stable and unstable periodic orbits in the one-dimensional lattice ϕ^4 theory*. Phys. Rev. E 94, 042209 (2016).

[4] J.-G. Caputo, A. Knippel and E. Simo, *Oscillations of networks: the role of soft nodes*. J. Phys. A: Math. Theor. 46 035101 (2013).

[5] A. C. Scott, *Encyclopedia of nonlinear science*. Ed., Routledge (Taylor and Francis) (2005).

Proceedings of WANCSA 2017
Normandie University, Le Havre, France - July 3-4, 2014

EXPLORING SOFT GRAPHS

Jean-Guy CAPUTO and Arnaud KNIPPEL

[1]

Keywords. Laplacian matrix, spectral graph theory, miscible flows on networks

Abstract

We are interested in graphs whose graph laplacian have an eigenvector with a null component. These null components play an important role when the graph Laplacian is used to describe miscible flows on a network. On these null components, any action, control or observation of the system is impossible; because they are so important it is useful to detect them in general networks.

The graph laplacian is the matrix of node degrees minus the adjacency matrix : we refer to [3] for definitions and results on graph spectra. In a previous work [1] we called *soft node* a vertex corresponding to such a component. In the case of a multiple eigenvalue, any component of an eigenvector may be zero and we call *absolute soft node* a vertex with value zero for all eigenvector in the subspace.

Here we call λ-*soft graphs* graphs with a soft node for an eigenvalue λ. We present a classification [2] of λ-soft graphs containing up to 6 nodes, as well as some particular classes of graphs, sorted by value of λ. This shows a structure within each λ-soft set with transformations connecting its members. This suggests that we can build soft graphs and find eigenvectors with soft nodes combinatorially.

Acknowledgements

This work is part of project XTerM, funded with the support from the European Union with the European Regional Development Fund (ERDF) and from the Regional Council of Normandie.

References

[1] J-G Caputo and A. Knippel and E. Simo, Oscillations of networks: the role of soft nodes, *Journal of Physics A: Mathematical and Theoretical* **46** (2013) 18pp.

[2] J-G Caputo and A. Knippel, Classification of λ-soft graphs, *technical report* (2017).

[3] D. Cvetkovic and P. Rowlinson and S. Simic, *An Introduction to the Theory of Graph Spectra*, London Mathematical Society Student Texts (No. 75), (2001).

[1] Jean-Guy CAPUTO and Arnaud KNIPPEL are with Laboratoire de Mathématiques, INSA de Rouen,
Normandie Université, 76801 Saint-Etienne du Rouvray, France.
E-mails: caputo@insa-rouen.fr, arnaud.knippel@insa-rouen.fr

Proceedings of WANCSA 2017
Normandie University, Le Havre, France – July 4-5, 2017

Berth Allocation Problem in an Automotive Transshipment Terminal

S. Benmansour, I. Diarrassouba, H. Dkhil and A. Yassine

1

Abstract

In this work, we study the berth allocation problem in the automotive transshipment terminal which operates in Le Havre port. Automotive transshipment terminals, also called Ro-Ro (i.e. Roll-on/Roll-off) terminals form a link in the transport chain for transshipment and temporary storage of cars. The ships arrive to and depart from the terminal for transferring cars in a given planning period. These ships must be assigned to berthing positions under some spatial and temporal constraints. Spatial constraints (i.e. allowable draft, length feasibility and ramp type) restrict the feasible berthing positions of ships while temporal constraints (i.e. availability of berthing positions and car drivers) restrict the berthing and departure times of ships. After berthing, each ship is handled by a team of drivers who are responsible of the transportation of the cars from the quay to their parking slots and vice-versa.

The main objective here is to minimize of the total waiting and handling time of the ships. The handling time (the unloading and loading time of cars) depends on several parameters. In this work, we explicitly express this time in terms of the distance traveled by the cars to be transferred (for unloading and loading) between the possible berthing positions and the parking slots, the total number of cars that has to be transferred, and the number of drivers assigned to the ship. This expression is realistic since it takes into account the main characteristics of Le Havre port Ro-Ro terminal. We also implement a mixed integer programming formulation of the problem and solve it using CPLEX 12.2. The instances used in the test set are based on realistic data and use the handling time model presented before.

Then, we investigate other operational goal which is the minimization of the car flow congestion within the terminal.

Authors are with Laboratory of Applied Mathematics of Le Havre, Normandie Université, ULH, 76600 Le Havre, France. E-mails: ibrahima.diarrassouba@univ-lehavre.fr, adnan.yassine@univ-lehavre.fr, and hamdi.dkhil@univ-lehavre.fr

Keywords. Berth allocation, automotive transshipment terminal, integer linear programming, handling ship time, traveled distance.

Figure: Automotive terminal, port of Le Havre

Acknowledgment

The research for this work was supported, in part, by the Natural Sciences and Engineering Research Council of Canada. This work is co-financed by the European Union with the European Normandy Regional Development Fund (ERDF) and by the Normandy Regional Council.

References

[1] Daofang Changa, Zuhua Jiang, Wei Yan, Junliang He ,Integrating berth allocation and quay crane assignments (2010), Transportation Research Part E: Logistics and Transportation Review, Volume 46, Issue 6, November 2010, Pages 975–990

[2] Yuquan Du, Qiushuang Chen, Xiongwen Quan, Lei Long, Richard Y.K. Fung, Berth allocation considering fuel consumption and vessel emissions (2011), Transportation Research Part E: Logistics and Transportation Review, Volume 47, Issue 6, November 2011, Pages 1021-1037

[3] Giovanni Giallombardo, Luigi Moccia, Matteo Salani, Ilaria Vacca, Modeling and solving the Tactical Berth Allocation Problem (2009), Transportation Research Part

B: Methodological, Volume 44, Issue 2, February 2010, Pages 232-245

[4] Dongsheng Xu, Chung-Lun Li, Joseph Y.-T. Leung , Berth allocation with time-dependent physical limitations on vessels (2012), European Journal of Operational Research, Volume 216, Issue 1, 1 January 2012, Pages 47-56

[5] Cheong, C.Y., Tan, K.C., Liu, D.K. et al , Multi-objective and prioritized berth allocation in container ports (2010), Annals of Operations Research, November 2010, Volume 180, Issue 1, Pages 63–103

[6] Katja Buhrkal, Sara Zuglian, Stefan Ropke, Jesper Larsen, Richard Lusby, Models for the discrete berth allocation problem: A computational comparison (2011), Transportation Research Part E: Logistics and Transportation Review, Volume 47, Issue 4, July 2011, Pages 461-473

[7] Victor Hugo Barros, Tarcísio Souza Costa, Alexandre C.M. Oliveira, Luiz A.N. Lorena , Model and heuristic for berth allocation in tidal bulk ports with stock level constraints, Computers & Industrial Engineering, Volume 60, Issue 4, May 2011, Pages 606-613

[8] Blazewicz, J. and Cheng, T. C. E. and Machowiak, M. and Oguz, C., Berth and Quay Crane Allocation: A Moldable Task Scheduling Model (2011). Journal of the Operational Research Society, July 2011, Vol. 62, Issue 7, Pages 1189-1197, 2011.

[9] Der-Horng Lee, Jiang Hang Chen, Jin Xin Cao, The continuous berth allocation problem: A greedy randomized adaptive search solution (2010), Transportation Research Part E: Logistics and Transportation Review, Volume 46, Issue 6, November 2010, Pages 1017-1029

Proceedings of WANCSA 2017
Normandie University, Le Havre, France - July 3-4, 2017

MULTIPLE HOPF BIFURCATIONS IN COUPLED NETWORKS OF PLANAR SYSTEMS

Guillaume Cantin, M.A. Aziz-Alaoui, Nathalie Verdière, Valentina Lanza *

Abstract. In this communication, we study coupled networks built with non-identical instances of a dynamical system exhibiting a Hopf bifurcation. We first show how the coupling generates the birth of multiple limit cycles. Next, we project those coupled networks in the real plane, and construct a polynomial Hamiltonian system of degree n, admitting $O(n^2)$ non-degenerate centers. We explore various perturbations of that Hamiltonian system and implement an algorithm for the symbolic computation of the Melnikov coefficients.

Keywords. Limit cycle, Hopf bifurcation, Hamiltonian system, Melnikov coefficients, coupled network.

1 Sequence of Hopf bifurcations in a directed chain of oscillators

Let us consider a directed chain of oscillators, built with the normal form of a Hopf bifurcation

$$\dot{\rho} = \rho(\lambda - \rho^2), \quad \dot{\theta} = 1, \tag{1}$$

where $(\rho,\ \theta)$ denote the polar coordinates of a generic point $(x,\ y)$ in $\mathbb{R}^2$. The whole coupled network is given by

$$\begin{cases} \dot{\rho}_1 = \rho_1(\lambda_1 - \rho_1^2) - \varepsilon\rho_1 \\ \dot{\rho}_k = \rho_k(\lambda_k - \rho_k^2) + \varepsilon\rho_{k-1} - \varepsilon\rho_k, 2 \leq k \leq n-1 \\ \dot{\rho}_n = \rho_n(\lambda_n - \rho_n^2) + \varepsilon\rho_{n-1}. \end{cases} \tag{2}$$

We consider that the cells have the same angular velocity, that is $\dot{\theta} = 1$, so we omit it in the equations of the network. For $n = 3$ and $\lambda_3 < 0 < \lambda_1 < \lambda_2$, in absence of coupling ($\varepsilon = 0$), cells 1 and 2 each admit one unstable equilibrium point, and one stable limit cycle whose respective radius $\bar{\rho}_1$, $\bar{\rho}_2$ satisfy $\bar{\rho}_1 < \bar{\rho}_2$. Cell 3 admits a unique stable equilibrium point. If the coupling strength ε weakly increases, we observe the appearance of a second cycle in cell 2, and simultaneously the appearance of two different cycles in cell 3. If ε keeps increasing, the cycle of greater radius first vanishes, and finally the other cycle vanishes too. Finally, the three cells present the same dynamic only for quite large values of ε. The bifurcation diagrams for cells 2 and 3 are depicted in Figure 1. This shows that a very simple network can also generate new limit cycles.

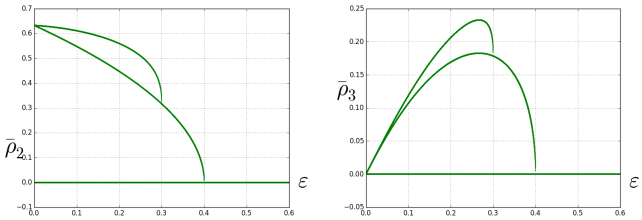

(a) (b)

Figure 1: Bifurcation diagrams for a three non identical cells directed chain.

In order to prove that the chain exhibits this sequence of Hopf bifurcations, we can make a local analysis based on the calculation of the first Lyapunov coefficient in the Poincaré normal form of the Hopf bifurcation [2, 4]. After basic computations, the first Lyapunov coefficient is given by

$$\ell_1(\mu) = -\frac{(2\delta + 3\mu)^2}{(\lambda_1 - \mu)^2}, \tag{3}$$

where $\delta = \lambda_2 - \lambda_1$ measures the difference of the dynamics of each node, and $\mu = \lambda_1 - \varepsilon$ is a translation of the coupling strength introduced in order to lighten the computations. In particular, we have $\ell_1(0) = \frac{-4\delta^2}{\lambda_1^2}$, thus the Hopf bifurcation that occurs in the network is supercritical, and degenerates into a Bautin bifurcation point if $\lambda_1 = \lambda_2$.

A longer chain can present a greater number of Hopf bifurcations. Such coupled networks have been applied to the study of neural networks or electric circuits networks [5]. It is remarkable that the number of limit cycles increases, but the degree of the polynomial involved in the system (2) is constant. In the following, we investigate the effect of projecting such a coupled network in the real plane.

*Laboratoire de Mathématiques Appliquées du Havre, Normandie University, Le Havre, France. E-mails: guillaumecantin@mail.com, aziz.alaoui@univ-lehavre.fr, nathalie.verdiere@univ-lehavre.fr, valentina.lanza@univ-lehavre.fr

2 Near-hamiltonian planar polynomial systems of degree n admitting n^3 limit cycles

In this section, we consider a Hamiltonian system admitting n^2 centers, and build a perturbation of that system. We show some examples for which the perturbed system admits n^3 limit cycles. To that aim, we introduce the following Hamiltonian system:

$$(\Sigma_{n,m}) \quad \begin{cases} \dot{x} = E_y \\ \dot{y} = -E_x, \end{cases} \tag{4}$$

with $n, m \in \mathbb{N}^*$,

$$E = \sum_{k=1}^{m} E_k \prod_{\substack{l=1 \\ l\neq k}}^{m} (x^2 + y^2 - \rho_l^2)^2, \tag{5}$$

where $\rho_1 < \rho_2 < \cdots < \rho_m$,

$$E_k = \frac{1}{2} \prod_{i=1}^{n} \left[(x - x_{i,k})^2 + (y - y_{i,k})^2 \right], \tag{6}$$

with $x_{i,k} = \rho_k \cos \frac{2i\pi}{n}$ and $y_{i,k} = \rho_k \sin \frac{2i\pi}{n}$.

Proposition 2.1. *For any $n, m \in \mathbb{N}^*$, the system $(\Sigma_{n,m})$ is Hamiltonian, invariant under rotation of center $(0,\ 0)$ and angle $\frac{2\pi}{n}$. Furthermore, it is polynomial of degree $O(n+m)$, and it admits $n \times m$ non-degenerate centers at $(x_{i,k},\ y_{i,k})$, $1 \le i \le n$, $1 \le k \le m$.*

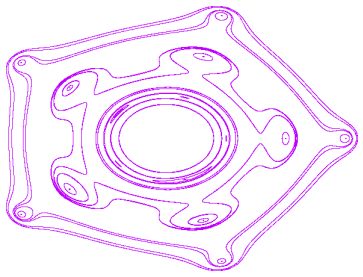

Figure 2: Energy levels of $(\Sigma_{5,3})$.

Now the difficult question is to find a polynomial perturbation of $(\Sigma_{n,m})$, of low degree, so that each center bifurcates into a given number a limit cycles. Thus we introduce for $\varepsilon > 0$ and $r \in \mathbb{N}^*$ the near-Hamiltonian system:

$$\left(\Sigma^{\varepsilon}_{n,m,r}\right) \quad \begin{cases} \dot{x} = E_y + \varepsilon P(x, y, \delta) \\ \dot{y} = -E_x + \varepsilon Q(x, y, \delta), \end{cases} \tag{7}$$

with

$$P(x, y, \delta) = \sum_{k=1}^{m} P_k(x, y, \delta) \prod_{\substack{l=1 \\ l\neq k}}^{m} (x^2 + y^2 - \rho_l^2), \tag{8}$$

where

$$P_k(x, y, \delta) = \sum_{i=1}^{n} -\sin \tfrac{2i\pi}{n} p_k \left(-\sin \tfrac{2i\pi}{n} x + \cos \tfrac{2i\pi}{n} y \right) \times \Big[\prod_{\substack{j=1 \\ j\neq i}}^{n} \left(-\sin \tfrac{2j\pi}{n} x + \cos \tfrac{2j\pi}{n} y \right) \Big],$$

and $p_k(u) = \sum_{s=0}^{r} \delta_{k,s} u^{2s+3}$ for $1 \le k \le m$.

Proposition 2.2. *For any $n, m, r \in \mathbb{N}^*$, the near-Hamiltonian system $\left(\Sigma^{\varepsilon}_{n,m,r}\right)$ is polynomial of degree $O(n + m + r)$.*

Finally, we present some examples for which we have computed the Melnikov coefficients [1] at each non-degenerate center, in order to show that $\left(\Sigma^{\varepsilon}_{n,m,r}\right)$ can admit $n \times m \times r$ limit cycles (see Table 1). It is a work in progress to prove it in the general case. Such a general theorem would constitute a new lower bound for Hilbert's number, that is $H(n) \ge O(n^3)$ (see [3] and the references therein).

Table 1: Some examples of system $\left(\Sigma^{\varepsilon}_{n,m,r}\right)$ admitting $n \times m \times r$ limit cycles.

n	m	r	Number of limit cycles
3	2	2	12
3	3	3	27
3	3	4	36
3	4	3	36
3	4	4	48
3	5	3	45
5	2	2	20
5	3	2	30

References

[1] M. Han, J. Yang, and P. Yu. Hopf bifurcations for near-hamiltonian systems. *International Journal of Bifurcation and Chaos*, 19(12):4117–4130, 2009.

[2] B. Hassard and Y. Wan. Bifurcation formulae derived from center manifold theory. *Journal of Mathematical Analysis and Applications*, 63(1):297–312, 1978.

[3] Y. Ilyashenko. Centennial history of hilbert's 16th problem. *Bulletin of the American Mathematical Society*, 39(3):301–354, 2002.

[4] Y. Kuznetsov. *Elements of Applied Bifurcation Theory*. Applied Mathematical Sciences. Springer New York, 2004.

[5] C. Zhang, B. Zheng, and L. Wang. Multiple hopf bifurcations of three coupled van der pol oscillators with delay. *Applied Mathematics and Computation*, 217(17):7155–7166, 2011.

Proceedings of WANCSA 2017
Normandie University, Le Havre, France - July 3-4, 2017

MATHEMATICAL AND NUMERICAL STUDY OF NETWORKS OF HODGKIN-HUXLEY REACTION-DIFFUSION SYSTEMS

A. Balti, B. Ambrossio and M.A. Aziz-Alaoui *

Abstract. In this work, we consider the networks of Hodgkin-Huxley model. We give a mathematical and numerical analysis of coupled reaction-diffusion Hodgkin-Huxley type. Thus, we used the semi-group theory for proving the existence and the uniqueness of solutions. And we show the existence of global solutions. Then, we use the method of invariant regions, we prove the existence of the global attractor in $C(\bar{\Omega})$. For the numerical simulation, we used a method of "splitting" for manipulation of nonlinear terms. We explore some examples of the bifurcation phenomena and propagation of bursting oscillations through one and two coupled Hodgkin-Huxley systems.

Keywords. Hodgkin Huxley model. Complex Dynamical Systems. Reaction-Diffusion Systems

General description

The general network of Hodgkin-Huxley model (HH) with duffision reads as:

$$\begin{cases} C\dfrac{\partial V_i}{\partial t} = \Delta V_i + I - [\overline{g}_{Na} m_i^3 h(V_i - E_{Na}) + \\ \qquad \overline{g}_K n_i^4 (V_i - E_K) + \overline{g}_L (V_i - E_L)] + \\ \qquad H_i(V_1, ..., V_N), \\ \dfrac{\partial n_i}{\partial t} = \alpha_n(V_i)(1 - n_i) - \beta_n(V_i) n_i, \\ \dfrac{\partial h_i}{\partial t} = \alpha_h(V_i)(1 - h_i) - \beta_h(V_i) h_i, \\ \dfrac{\partial m_i}{\partial t} = \alpha_m(V_i)(1 - m_i) - \beta_{m_i}(V) m_i, \end{cases} \tag{1}$$

in a bounded domain $\Omega \in \mathbb{R}^n$ and with homogeneous Neumann conditions and where

$u := (V_i)_{0...N}$, and $v := (n_i,\ m_i,\ h_i)_{0...N}$

$$H_i(u) = \sum_{j \in \{1,...,N\}} \alpha_{ij}(S - u_i)\Gamma(u_j) \text{ case of nonlinear coupling} \tag{2}$$

and

$$\Gamma(s) = \frac{1}{1 + \exp^{-\lambda(s-\theta))}}$$

with $S, \lambda > 0, \theta \in \mathbb{R}$, $\alpha_{ij} \geq 0$.

Existence and uniqueness of solution and his asymptotic behaviour

We use the semigroup theory and the fixed point theorem then we have this result of existence and uniqueness global solution of (1).

Theorem 0.1. *For all initial conditions* $(Vi(0),\ ni(0),\ mi(0),\ hi(0)) \in C(\bar{\Omega})^{4n}$ *such that* $\forall x \in \Omega,\ n_i(0,\ x),\ m_i(0,\ x),\ h_i(0,\ x) \in [0,\ 1]$, *there exists a unique solution* $U \in C([0,\ +\infty[,\ C(\bar{\Omega})^{4n}) \cap C^1(]0,\ +\infty[,\ C(\bar{\Omega})^{4n})$ *of (1).*

Proof

Let Ω be a bounded domain in $\mathbb{R}^n$.
$C(\bar{\Omega})$ the space of continuous functions defined on Ω.
We note $E = (C(\bar{\Omega})^N, \|.\|_E)$ is a Banach spaces. Where $\|f\|_E = \sum_{1,N} max_{x \in \Omega} |f_i(x)|$.

First we consider the homogeneous problem. Thus, the homogeneous solution with an initial condition U_0 is given

$$U_H = S(t)U_0, \tag{3}$$

where $(S(t))_t$ is analytic semigroup, see [1, 2]. In now, for $T > 0$ we define the space $F = (C[0, T[, E)$, where $\|u\|_F = sup_{[0,T[} \|u\|_E$. F is a Banach space. Then, we apply the fixed point theorem to show the existence of mild solution, See [1].

□

For the asymptotic behaviour, we use the invariant region technique and the classical some properties of analytic semigroup then we show the existence of a global attractor of (1).

Theorem 0.2. *The semiflow* $T(t)$ *associate with system (1) admits a global attractor* $\mathbb{A}$.

Proof

The system (1) has an invariant region. It's easy to prove that $n_i(t,\ x),\ m_i(t,\ x),\ h_i(t,\ x) \in [0,\ 1],\ \forall t \in$

*Balti, Ambrossio and Aziz-Alaoui : Normandie Univ, France; ULH, LMAH, F-76600 Le Havre; FR CNRS 3335, ISCN, 25 rue Philippe Lebon 76600 Le Havre, France. E-mails: aymen.balti@univ-lehavre.fr, benjamin.ambrossio@univ-lehavre.fr, aziz.alaoui@univ-lehavre.fr

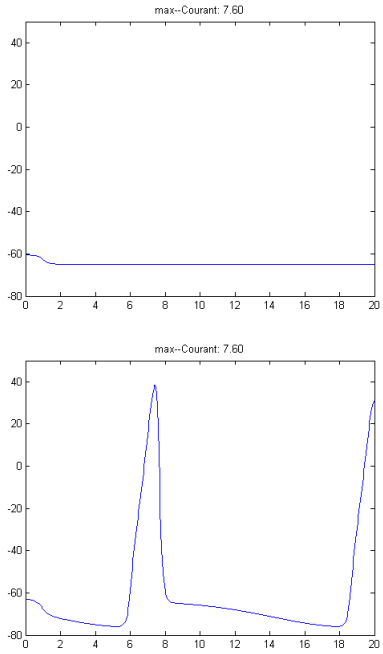

Figure 1: Representation of the $V(x,t)$ for $I = 7.6$. We have the coexistence of two attractive solutions.

$[0, \ +\infty[$. For the potential variables, we use the property of dissipativity, see [1, 2]. We can find tow Constant values V_{min} and V_{max}, such that, $V_i \in [V_{max}, V_{max}]$. The existence of an invariant region give the global existence in time of solutions for our reaction-diffusion system (1).

We denote by $T(t)$ the semi-groupe associate with system (1). We can write $T(t) = T_1(t) + T_2(t)$. Then, the main idea is to prove that the semi-groupe $T_1(t)$ is compact operator for $t > t_0$ and the semi-groupe $T_2(t)$ near to zero for large time, see [1, 2].

□

Numerical results

We deal with system (1) with $N = 1$. We have proceeded to numerical simulations in the interval $[0, \ 10]$. using our matlab program with a uniform finite difference scheme in space and a splitting method integration in time, see [1, 2]. So, we explore the interesting phenomena: Coexistence of two attractive solutions see the figure 1 and the propagation of busting oscillations see the figure 2.

Conclusion

We have proved existence and uniqueness of solutions as well as the existence of invariant region and of the attractor in the space of continuous functions. We have also exhibited bifurcation phenomena and propagation of bursting oscillations.

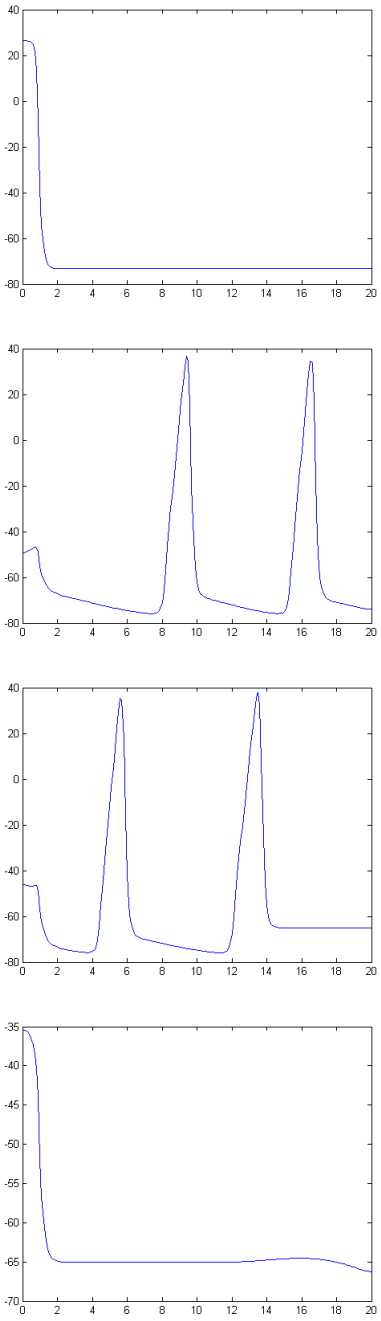

Figure 2: Propagation of burst Oscillation for $I = 134$. We represente the solutions $V(x,t)$ for different instants of time, $t = 51, 100, 320, 2975$.

In future works, we aim to develop theoretical tools to describe and analyze these phenomena.

References

[1] A. BALTI, *Modélisation mathématique et analyse de réseaux complexes d'interaction de Hodgkin-Huxley, application en neuroscience* , PhD Thesis, Le Havre Normandie University, 2016.

[2] B. Ambrosio, M.A. Aziz-Alaoui, A. Balti, (2017) *Propagation of bursting oscillations in coupled non-homogeneous Hodgkin-Huxley Reaction-Diffusion systems*, To appear in Differential Equations and Dynamical Systems. DOI:10.1007/s12591-017-0366-6

Proceedings of WANCSA 2017
Normandie University, Le Havre, France - July 4-5, 2017

ENVIRONMENT IMPACT ON POLIO DISEASE

C. Balde, M. Lam, A. Bah, S. Bowong, J.J. Tewa [*, †‡§]

Abstract. The aim of this study is to show how the environment contamination is influencial in the transmission dynamic of polio disease. A new deterministic model for the transmission dynamic of polio disease with environment contamination is disigned and rigourisly analysis. We compute the basic reproduction number $\mathcal{R}_0^{env}$ and show that whenever $\mathcal{R}_0^{env} < 1$ the disease free equilibrium is globally assymptotically stable (GAS). And when $\mathcal{R}_0^{env} > 1$ we show that the full model has a unique endemic equilibrium which is locally assymptotically stable(LAS). Then we compare this model to the deterministic model without environment contamination. We prove the same results occurs for the GAS of the disease free equilibrium and LAS of the endemic equilibrium whenever the corresponding basic reproduction number $\mathcal{R}_0$ is less than and more than unity respectively. Our finding suggests the contaminated environment plays a detrimental role on the transmission dynamics of polio disease. Further, we perform numerical simulations to support the theory.

Keywords. Poliovirus, environment contamination, human shedding rate.

*C. Balde, M. Lam are with Department of Mathematics, Faculty of Science and Technic, UCAD, Dakar (Senegal).

†A.Bah is with Department of Computer Engineering, National Advanced School of Engineering, UCAD, Dakar (Senegal).

‡S. Bowong is with Faculty of Science, University of Douala, Cameroon. E-mail: sbowong@gmail.com.

§J.Tewa is with National Advanced School of Engineering, University of Yaounde I.

Acknowledgements

The financial support of the CEA-MITIC from UGB-St louis (Senegal) is gratefully acknowledged.

Proceedings of WANCSA 2017
Normandie University, Le Havre, France - July 3-4, 2014

ANALYSIS OF AN EPIDEMIC MODEL ON A NETWORK

Jean-Guy CAPUTO, Arnaud KNIPPEL and Fatima MOUATAMIDE

[1]

Keywords. Epidemic propagation, miscible flows on networks, Laplacian matrix

Abstract

Networks or graphs are interesting tools for representing complex systems due to their abstract and flexible constructions. In epidemiology, graphs are used to model how an infection spreads: nodes can describe locations where individuals live and links represent the connections between them. Here, we analyze a KermacK-Mckendrick model on a geographical network; this yields a system of coupled differential equations involving the graph Laplacian of the network.

We study the influence of the different parameters and obtain a simple criterion for the onset of the epidemic. We show how the weights on the branches impact the propagation. Finally, in order to curb the epidemic we examine different vaccination strategies by acting locally on the parameters of the model. We illustrate these results on the network of the six major cities of Mexico and on a larger network containing the fourteen main cities of France.

Acknowledgements

This work is part of project XTerM, funded with the support from the European Union with the European Regional Development Fund (ERDF) and from the Regional Council of Normandie.

[1]Jean-Guy CAPUTO, Arnaud KNIPPEL and Fatima MOUATAMIDE are with Laboratoire de Mathématiques, INSA de Rouen,
Normandie Université, 76801 Saint-Etienne du Rouvray, France.
E-mails: caputo@insa-rouen.fr, arnaud.knippel@insa-rouen.fr, fatza.mouatamide@gmail.com

Proceedings of WANCSA 2017
Normandie University, Le Havre, France - July 4-5, 2017

TRANSMISSION PROBLEM IN POPULATION DYNAMICS

Alexandre Thorel *

Keywords. Population dynamics, Diffusion equation, Semigroups, Landau-Ginzburg free energy functional.

1 Abstract

We study a transmission problem, in population dynamics, set in a cylindrical open set Ω of form:

$$\Omega :=]a, b[\times \omega, \quad \text{with} \quad \Omega := \Omega_- \cup \Gamma \cup \Omega_+,$$

where $\Omega_- :=]a, \gamma[\times \omega$, $\Gamma := \{\gamma\} \times \omega$ and $\Omega_+ :=]\gamma, b[\times \omega$ with $\gamma \in \ ]a, b[\ \subset \mathbb{R}$ and $\omega \subset \mathbb{R}^{n-1}$.

In each habitat, we consider that there exists a population and its dispersal is model by the following generalized diffusion equation:

$$k\Delta^2 u - l\Delta u = f,$$

where $k, l > 0$. Here, the biharmonic term model the long range dispersion whereas the laplacian model the short range dispersion (see J.D. Murray [4]).

To study this problem, we use some techniques based on operational differential equations: sums of linear operators, fractional powers of operators, semigroups theory and interpolation theory (see M. Haase [2]), G. Dore & A. Venni [1] and H. Triebel [5]).

More precisely, we writes equations into fourth order operational equations in $X := L^p(\omega)$, $p \in \ ]1, +\infty[$, a complex Banach space.

Setting $(u(x))(y) := u(x, y)$ with $x \in \ ]a, b[$, $y \in \omega$ and Δ_y, the $n-1$-dimensional Laplace operator, we define $Au(x) := \Delta_y u(x)$ and $D(A)$ the domain of A which depends on considered boundary conditions. Then, we obtain problem (P)

$$(P) \begin{cases} (EQ) \begin{cases} u_-^{(4)}(x) + (2A - \frac{l_-}{k_-} I)u_-''(x) + (A^2 - \frac{l_-}{k_-} A)u_-(x) = f_-(x), & \text{a. e. } x \in \ ]a, \gamma[\\ u_+^{(4)}(x) + (2A - \frac{l_+}{k_+} I)u_+''(x) + (A^2 - \frac{l_+}{k_+} A)u_+(x) = f_+(x), & \text{a. e. } x \in \ ]\gamma, b[, \end{cases} \\ (BC) \begin{cases} u_-(a) = \varphi_1^-, \quad u_+(b) = \varphi_1^+, \\ u_-'(a) = \varphi_2^-, \quad u_+'(b) = \varphi_2^+, \end{cases} \\ (TC) \begin{cases} u_-(\gamma) = u_+(\gamma) \\ u_-'(\gamma) = u_+'(\gamma) \\ k_+ u_+^{(3)}(\gamma) + k_+ A u_+'(\gamma) - l_+ u_+'(\gamma) = k_- u_-^{(3)}(\gamma) + k_- A u_-'(\gamma) - l_- u_-'(\gamma) \\ k_+ u_+''(\gamma) + k_+ A u_+(\gamma) = k_- u_-''(\gamma) + k_- A u_-(\gamma). \end{cases} \end{cases}$$

We use the results of [3] to show that, on some hypotheses on data of problem (P), we can build solutions

$$u_- \in W^{4,p}(a, \gamma; X) \cap L^p(a, \gamma; D(A^2))$$

and

$$u_+ \in W^{4,p}(\gamma, b; X) \cap L^p(\gamma, b; D(A^2))$$

of this problem satisfying the boundary conditions of (P). Finally, we inverse an operational determinant to show that among previous couples (u_-, u_+), only one satisfies the transmission conditions. This couple is the unique solution of problem (P) which have the expected regularity. If A is a more general linear operator, under some hypotheses on A, this result stay true.

Acknowledgements

The research is supported by CIFRE contract 2014/1307 with Qualiom Eco company.

References

[1] G. Dore & A. Venni, *On the Closedness of the Sum of Two Closed Operator*, Math. Z., 196, 1987, pp. 189-201.

[2] M. Haase, *The Functional Calculus for Sectorial Operators*, Birkhauser, 2006.

[3] R. Labbas, S. Maingot, D. Manceau & A. Thorel, *On the regularity of a generalized diffusion problem arising in population dynamics set in a cylindrical domain*, Journal of Mathematical Analysis and Applications, 450, 2017, pp. 351-376.

[4] J.D. Murray, *Mathematical Biology II: Spatial Models and Biomedical Applications*, Third Edition, Springer, 2003.

[5] H. Triebel, *Interpolation theory, Function Spaces, Differential Operators*, North-Holland publishing company Amsterdam New York Oxford, 1978.

*Normandie Univ, UNIHAVRE, LMAH, FR-CNRS-3335, 76600 Le Havre, France. E-mails: alexandre.thorel@orange.fr

Proceedings of WANCSA 2017
Normandie University, Le Havre, France – July 4-5, 2017

Subgraph component polynomials of some compound graphs

Xiaoliang Xie, Yunhua Liao[1]

Abstract. Let G be a graph with n vertices and let $R_1, R_2, \mathrm{L}\ , R_n$ be distinct rooted graphs. The compound graph $G[R_1, R_2, \mathrm{L}\ , R_n]$ is obtained by identifying the root of R_i with the i-th vertex of G. Inspired by the study of community structure in connection networks, Tittmann, Averbouch and Makowsky introduce the subgraph component polynomial $Q(G; x, y)$, which counts the number of connected components in vertex induced subgraphs. The subgraph component polynomial contains several other polynomial invariants, such as the independence polynomial. Motivated by a result of Gutman on the independence polynomial of $G[R_1, R_2, \mathrm{L}\ , R_n]$, we extend the result for the subgraph component polynomial.

Keywords. Subgraph component polynomial; Independence polynomial; Compound graph; Cograph; Graph polynomials

1 Introduction

Throughout this paper, we will consider only graphs with no loops and multiple edges. Let $G = (V, E)$ be a finite and undirected graph with vertex set $V = V(G)$ and edge set $E = E(G)$. If $X \subseteq V$, then $G[X]$ is the subgraph of G spanned by X. $G - X$ we mean the subgraph $G[V - X]$, and we write shortly $G - v$, whenever $X = v$.

As usual, the complete graph on n vertices is denoted by K_n. The open neighborhood of a vertex v is the set $N_G(v) = \{w \in V(G) : vw \notin E(G)\}$, and the closed neighborhood $N_G[v] = N_G(v) \cup \{v\}$; if there is no ambiguity on G, we use N(v) and N[v], respectively. The disjoint union of the graphs G_1, G_2 is the graph $G = G_1 \cup G_2$ having as vertex set the disjoint union of $V(G_1), V(G_2)$, and as edge set the disjoint union of $E(G_1), E(G_2)$. For more standard definitions, we refer the reader to the text of Diestel [1]..

An independent set in G is a set of vertices no two of which are adjacent. Let Ind(G) be the set of all independent sets of G. Let s_k be the number of independent sets of cardinality k in a graph G with n vertices. The polynomial

$$I(G) = I(G; x) = \sum_{i=0}^{n} s_i x^i = s_0 + s_1 x + \mathrm{L}\ + s_n x^n$$

is called the independence polynomial [2]. Since its introduction in the early 1980s, the independence polynomial has been the focus of considerable research .

Let G be a graph with vertex set $V(G) = \{v_1, v_2, \mathrm{L}\ , v_n\}$. Let further $R_1, R_2, \mathrm{L}\ , R_n$ be distinct rooted graphs; the root of R_i is denoted by r_i. Then $G[R_1, R_2, \mathrm{L}\ , R_n]$ is the graph obtained by identifying the vertex v_i of G with the root r_i of R_i, simultaneously for see figure 1.

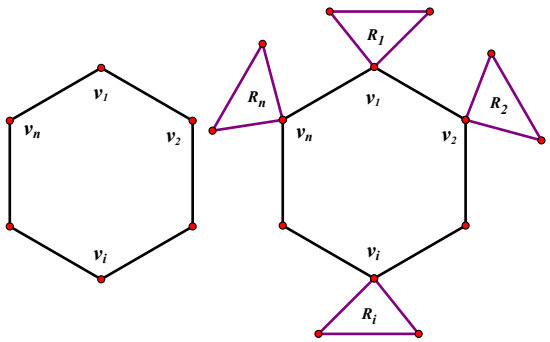

Figure 1 The construction of $G[R_1, R_2, \mathrm{L}\ , R_n]$

Gutman [3] determined the independence polynomial of $G[R_1, R_2, \mathrm{L}\ , R_n]$. Denote by R_i^{o} the graph obtained by deleting from R_i the root-vertex r_i and the edges incident to it. Denote by $R_i^{\bullet}$ the graph obtained by deleting from R_i the root-vertex r_i and the vertices adjacent to r_i and all the incident edges.

Xiaoliang Xie and Yunhua Liao are with Department of Mathematics, Hunan University of Commerce, Changsha, China. E-mails: 349600592@qq.com, 307156168@qq.com

Theorem 1 [3] Let A be an independent set of the graph G. Define

$$I(G[R_1, R_2, \cdots, R_n], x) = \sum_{A \in Ind(G)} x^{|A|} \prod_{i=1}^{n} I_i(A)$$

Then

$$I(G[R_1, R_2, \cdots, R_n], x) = \sum_{A \in Ind(G)} x^{|A|} \prod_{i=1}^{n} I_i(A)$$

The subgraph component polynomial $Q(G; x, y)$ has been first introduced in [4]. Its formal definition is the following. Let A be a vertex induced subgraph of G and k(A) denote the number of components of A. Let $q_{ij}(G)$ be the number of vertex induced subgraphs A with i vertices and j components. The subgraph component polynomial $Q(G; x, y)$ of G is defined as an ordinary generating function for these numbers:

$$Q(G; x, y) = \sum_{i=0}^{n} \sum_{j=0}^{n} q_{i,j}(G)\, x^i y^j.$$

2 Main result

Fist, we derive a new recursive relation for the subgraph component polynomial.

Theorem 2 Let G be a graph and $e = uv$ be an edge of G. Then

$$\begin{aligned} Q(G; x, y) &= Q(G - u; x, y) + Q(G - v; x, y) + xQ(G/e; x, y) \\ &- (1 + x)Q(G \dagger e; x, y). \end{aligned}$$

Then, we study the subgraph component polynomial of graph $G[R_1, R_2, \mathrm{L}\ , R_n]$.

Theorem 3. *For every vertex induced subgraph A of G define*

$$Q_i(A) = \begin{cases} Q(R_i^{\circ}) & \text{if } v_i \notin A; \\ \frac{1}{xy} Q(R_i^{\bullet}) & \text{if } v_i \in A. \end{cases}$$

Then

$$Q(G[R_1, R_2, \cdots, R_n]; x, y) = \sum_{A \subset G} x^{|A|} y^{k(A)} \prod_{i=1}^{n} Q_i(A).$$

Acknowledgment

This project was supported by the National Natural Science Foundation of China under Grant Nos. 11171102 and 11571101.

References

[1] R. Diestel, Graph Theory, in: Graduate Texts in Mathematics, Springer, NewYork, 2000.

[2] I. Gutman, F. Harary, Generalizations of the matching polynomials, Utilitas Mathematica, 24 (1983) 97-106.

[3] P. Tittmann, I. Averbouch, J. A. Makowsky, The enumeration of vertex induced subgraphs with respect to the number of components, European Journal of Combinatorics, 32 (2011) 954-974.

Index


LMAH


litis


LMI - EA 3226


cnrs
dépasser les frontières


RÉGION
NORMANDIE


MRT


SFBT


ISCN


UNESCO
United Nations
Educational, Scientific and
Cultural Organization
uniTwin
COMPLEX SYSTEMS
DIGITAL CAMPUS


Normandie - Mathématiques


xterm


Normandie Université


UNIVERSITÉ
LE HAVRE
NORMANDIE